7

Signals, Noise, and Thresholds

James C. Weaver and Martin Bier

CONTENTS

7.1 Signals, Detection, and Measurement

Measurement is a quantitative observation and well known to be of great importance to science. However, measurements involving biological systems are complicated by the complexity of cells and tissues, particularly if fields are expected to interact weakly and field-induced changes are found to be small. Some key parameters, for example, temperature coefficient of a measured quantity, may be inadequately characterized, and related quantities may be determined incompletely (e.g., measurement or modeling of the time-dependent temperature throughout the volume of the biological system being studied). Detection is a special case of measurement, that is, the measurement is so coarse that an observer can only distinguish between ''signal'' and ''no signal.''

Generally speaking, the smaller the change in an observed quantity (e.g., cell biomass) due to a stimulus (e.g., an applied electromagnetic field), the more difficult the experimental interpretation. There may be multiple candidate causes if small changes in biomass are found, for example, any of many growth-altering biochemical changes, unnoticed and uncharacterized temperature variations, or even changes in ambient light or mechanical vibration. In physical science a model can often be made of the experiment. This allows estimates of the influence of various quantities and parameters on the expected experimental outcome (change in observed quantity in response to a stimulus) and is valuable in the interpretation of experiments. Similar approaches to bioelectromagnetics should also be valuable.

Consider an illustrative measurement on a biological system: a population of microorganisms contained within a glass toroid. Application of an alternating magnetic field to a primary coil wrapped around one part of the toroid induces an alternating current. The induced current can be measured with a coil wound around part of the toroid. The induced current is related to the electrical conductivity of the aqueous electrolyte. The electrical conductivity of the extracellular medium changes when small, charged metabolites are excreted, and measurement of microbial metabolic activity can thus be accomplished electrically. First observed in 1899 by a nulling technique [1], electrical impedance detection of microorganisms has received significant attention as a measurement method [2,3]. A toroidal device has actually been explored as the basis for determining microbial activity [4], with metabolic acid production causing a change in extracellular ion concentration (activity) and therefore creating a change in the electrical conductivity of the extracellular medium. But complications may arise. If cytotoxic chemicals leach from the glass, there can be a time-dependent poisoning of microbial activity. Ambient temperature changes couple through the glass to create internal temperature variations that alter the conductivity. In short, because electrical conductivity change has more than one candidate cause, this measurement system lacks specificity. This also illustrates a basic challenge to measurement of effects of electromagnetic fields on biological systems, namely, demonstrating both a statistically significant change and convincing evidence that it is the field interaction with the biological system, not an associated competing influence, that is responsible for the observation.

7.2 Specificity

Specificity is a hallmark of biological interactions involving biochemicals. A cell contains a large number of coexisting molecules whose interactions are not spontaneous but are instead highly regulated. Enzymes can be highly specific in the reactions they catalyze. Antibodies and receptor–ligand binding are also often specific. However, interactions of electromagnetic fields with a biological system are rather general. Magnetic fields interact indirectly by inducing electric fields and directly through magnetically sensitive reactions [5] and through interactions with magnetic material. Such magnetic materials may be contaminant ferromagnetic particles in the human body [6] or they may be biologically synthesized magnetite granules [7,8]. Electric fields interact nonspecifically with charge and polarizable material. Thus, unlike ligand–receptor biochemical interactions, there are no molecular receptors that are highly specific for electromagnetic fields. Instead, magnetic and electric sensory systems interact broadly and can be regarded as nonspecific. Evolved sensory systems are rather special. To date, it appears that biological, electric and magnetic field reception is indeed accomplished by organized systems.

Lack of electromagnetic field specificity has important implications for interpreting experiments. If an experiment quantifies a change in an observed parameter, the cause of the change is not automatically known. Continuing the example of cell growth determination based on biomass measurement, if an increase in biomass (or cell number) is associated with a field exposure, then additional analysis is needed to determine whether this change is due directly to the field or is instead due to interfering influences such as temperature change or biochemical concentration changes.

The challenge of specificity is not limited to weakly interacting fields. Consider the case of strong, electroporating fields *in vivo*, for which the motivation is local tumor treatment

or gene therapy. Strong fields can generate tissue movement by stimulating muscles and possibly also by bulk tissue polarization forces. Tissue motion can itself create membrane openings, and these can lead to biochemical transport [9–11]. Thus, observation of molecular uptake associated with electrical pulsing does not by itself show that electroporation is responsible. Specificity is an issue.

7.3 Signal-to-Noise Ratio

We adopt a recent discussion of the signal-to-noise ratio (S/N) for experiments with biological systems exposed to weakly interacting electromagnetic fields [12]. The observed quantity is x. For bioelectromagnetics experiments, examples of x include a local or spatially averaged transmembrane voltage change, temperature rise at a particular site, radioactivity of an incorporated unstable isotope, specific enzyme activity, intracellular calcium ion concentration, cell biomass, etc. Typically, experiments obtain data that can be characterized by their means and standard deviations, often presented as a bar chart. One bar of each bar pair represents the control result, and the other bar represents the exposed result. Each bar height represents the mean value, and the error bar is usually the standard deviation. (In some cases the error bars instead represent the standard error, that is, the uncertainty in the mean, rather than the standard deviation, but generally a report states which is being used.) Bar charts present a concise summary of an investigator's knowledge of the underlying natural distributions. The measured mean and standard deviation of the control distribution can be defined to be $\bar{x}_{\text{con}}$ and σ_{con}, respectively. Similarly, $\bar{x}_{\text{exp}}$ and σ_{exp} are the observed mean and standard deviation of the exposed distribution.

When repeating the same experiment and doing the same measurement many times over, one generally finds a Gaussian distribution of outcomes. This is because in a complex system there are many variables and sources of inaccuracy that are not under the control of the experimentalist. For the cumulative effect of all these imprecisions the central limit theorem becomes applicable. This theorem says that with many independent stochasticities involved, the outcome will be a Gaussian distribution [13]. As an example of this theorem in practice, do 100 coin tosses and record the number N of ''heads.'' Repeat this experiment many times. The result will converge to a Gaussian distribution of N that is centered around 50.

The threshold for a field exposure effect occurs under conditions of detection, that is, the minimum change of x that is discernable using generally accepted statistical criteria. This is equivalent to determining whether or not the control statistical distribution and the exposed distribution are distinguishable (significantly different by accepted criteria). This requires sufficiently precise knowledge of the statistical distribution parameters. Increasing the number of determinations of the natural distribution generates more precise knowledge of its parameters. For example, if an investigator carries out a number, m_{con}, of determinations of x_{con} and another number, m_{exp}, of determinations of x_{exp}, then the empirically determined values can be reported as

$$x_{\text{con}} = \bar{x}_{\text{con}} \pm \frac{\sigma_{\text{con}}}{\sqrt{m_{\text{con}}}} \quad \text{and} \quad x_{\text{exp}} = \bar{x}_{\text{exp}} \pm \frac{\sigma_{\text{exp}}}{\sqrt{m_{\text{exp}}}} \tag{7.1}$$

The ratio $\sigma/\sqrt{m}$ actually represents the aforementioned standard error. Increasing the number of determinations reduces the standard error and the ensuing uncertainty in the mean. However, it does not decrease the standard deviation, σ_{exp}, of the underlying distribution, which is assumed unperturbed by the measurement process.

As the means $\bar{x}_{con}$ and $\bar{x}_{exp}$ become better known through more determinations, the potential distinguishability of the two distributions increases. The p-value of the experiment is often reported as a measure of this distinguishability. The p-value is the probability that the two means would be found to be as different as observed (or even more different) purely because of random variability. For example, $p = 0.01$ indicates that there is only a 1% chance that the difference between the control mean and the exposed mean would be due to the (assumed) random variability of the measured quantity, namely, the standard deviation [14]. After an investigator completes an experiment and finds a reasonably small p-value (.01 and .05 are widely used values), it is a common practice for the investigator to report that an effect due to the field exposure has occurred. However this assumes specificity, namely, that the field exposure rather than an associated competing influence is responsible. Indeed, a small p-value supports an effect of some sort but not necessarily one due to the field during the exposure. Additional analysis that considers other competing influences such as temperature variations, vibrations, and chemical concentration variations [15,16] is required for that conclusion.

Bioelectromagnetics experiments with weakly interacting fields typically involve determination of changes with respect to background values of, for instance, transmembrane voltage, fluorescence intensity, enzyme activity, or cell number. Observed changes in ''exposed'' relative to ''control'' are generally small. At the other extreme, strongly interacting fields create large changes with respect to background, for example, molecular uptake by electroporation (see Chapter 9 on electroporation in Ref. [127]). For the ''weakly interacting'' situation the uncertainties (error bars) are about the same for exposed and control. However, there is another figure of merit, distinct from the p-value, namely, an empirically determined signal-to-noise ratio $(S/N)_{obs}$, which is associated with the observation and which is presumed due to the underlying statistical distributions for the control and exposed cases. Classical detection theory shows that the associated distributions are expected to be Gaussians [17].

In continuation of a recent discussion [12], we consider the observed signal (S_{obs}) to be the difference between the control and the exposed means, and the observed noise (N_{obs}) as the standard deviation of the control distribution [17]. This yields

$$S_{obs} = \bar{x}_{exp} - \bar{x}_{con} \quad \text{and} \quad N_{obs} = \sigma_{con} \tag{7.2}$$

so that the empirically determined signal-to-noise ratio is the magnitude of

$$(S/N)_{obs} = \frac{\bar{x}_{exp} - \bar{x}_{con}}{\sigma_{con}} \tag{7.3}$$

Like the p-value $(S/N)_{obs}$ is a measure of the distinguishability of the two distributions. However, unlike the p-value, the signal-to-noise ratio is an inherent characteristic of the biological system, its environment, and a particular field exposure and does not depend on the number of determinations. In this view, S_{obs} is the observed change and is assumed to be a measure of the strength of the perturbation to the biological system by the field exposure. N_{obs} is a measure of the natural variability in the system for the conditions of the experiment. In the absence of an exposure, N_{obs} provides the appropriate scale to gauge the strength of S_{obs}.

$(S/N)_{obs}$ is based only on experimental determinations of x. However, in many cases the field exposure is believed to *indirectly* alter x. According to this general hypothesis, the field exposure affects one or more molecular-level biochemical processes through physical interactions. In this sense, the exposure is creating a ''primary'' molecular change, which is then amplified through a biochemical cascade that creates a downstream change. It is this downstream change that is eventually measured. The signal-to-noise ratio cannot be increased by the amplification process. Later in this chapter, we will describe how amplification generally adds noise to a signal.

7.4 Detection Criteria

The criterion $(S/N) \leq 0.1$ is a very conservative basis for ruling out a particular class of biophysical mechanism for a given field exposure. Similarly, the criterion $(S/N) \geq 10$ is a conservative basis for ruling in a candidate biophysical mechanism for a given exposure, retaining that biophysical mechanism hypothesis for further evaluation. This approach provides a quantitative basis for rejecting or accepting hypothetical biophysical mechanisms as candidate explanations for an experimental measurement. The traditional choice $(S/N) \approx 1$ is a useful but somewhat arbitrary dividing line, which indicates conditions for which an effect might appear. $(S/N) \leq 0.1$ and $(S/N) \geq 10$ provide criteria for stronger conclusions, allowing rejection or provisional retention of a biophysical mechanism hypothesis.

We should recognize that thresholds are defined by generally accepted statistical criteria. The widely used p-values of .01 and .05 are examples of such generally accepted statistical values. In the case of signal-to-noise ratios, a commonly accepted value is $(S/N) \approx 1$, where the approximately equal symbol denotes the imprecision. Specifically, if (S/N) (empirical or theoretical) exceeds 1, then the threshold is viewed as being exceeded. Similary, if (S/N) is less than 1, the response is interpreted as subthreshold. Clearly, it makes little sense to take a strong position if (S/N) is close to 1. But, as noted above, if the signal-to-noise ratio is significantly greater or less than 1, then some confidence can be attached to the result. In short, a threshold is imprecise but nevertheless a useful guide.

7.5 Equilibrium Noise

In this section we will examine how Brownian noise, the simple random motion of molecules due to thermal agitation, interferes with the coupling of an electromagnetic field to a biochemical system. Some organisms have evolved an ability to sense and effectively ''measure'' electric and magnetic fields. We will see that the thermal noise that a signal has to compete against sets fundamental limits on detectability. We will also see how evolution has come up with structures to optimize the signal-to-noise ratio in sensory perception.

Fish generally carry a small dipolar field relative to the water that they swim in. Sharks, skates, and rays have developed special organs to detect such fields [18,19] and they use this ability to pinpoint the position of their prey when they get close and the water is too turbulent to rely on smell. To be effective, the shark should be able to sense its prey

instantaneously. So, for the signal not to be mistaken for Brownian noise and for Brownian noise not to be mistaken as a signal, a signal should carry an energy that is significantly larger than *kT*. *kT* constitutes the average energy in the thermal noise band [20]. This baseline criterion already works to explain some of the physiology of the electric sensing organs. The electric fields are picked up by the ampullae of Lorenzini. These ampullae terminate at pores in the skin around the fish's head. They are enclosed in a highly resistive material and are filled with a very conductive gel. The eventual setup is equivalent to an electrical wire with no voltage drop inside. These ampullae are, furthermore, well insulated against electrical noise that originates from the fish's own physiology. Two pores that are about 10 cm apart on the surface of the fish's head can, on the inside ends, be separated only by a few nanometers. A field of 500 nV/m can be detected. Two pores that are 10 cm apart on the surface could thus transfer 50 nV into a transmembrane potential.

By having a lot of ion channels that are sensitive to such small voltage variations, the thermal noise can be effectively averaged out. With N ion channels instead of just one, N times as much signal strength is picked up. The thermal noise at each channel is independent of that at any other channel. The noise is zero-average and the noise variances are added up for N channels. So the average noise amplitude will be only $\sqrt{N}$ times as large if N channels are involved instead of one. After detection, the fish has to amplify this signal to the millivolt range that the nervous system operates with. Amplifier noise constitutes a problem that builders of electric circuits have dealt with for decades. Amplifier noise is nonequilibrium noise, and we will discuss it in the next section. Over the past decade, researchers have built up a good and detailed understanding of the physiology [21] and physics [22,23] of the fishes' amplification system.

Many animal species have the ability to detect the geomagnetic field. Two mechanisms have been proposed for magnetosensitivity. The first mechanism involves chemical transitions that are sensitive to external magnetic fields. Upon excitation by light, many polyatomic molecules will start transiting between the singlet ground state, the singlet excited states, and the excited triplet state. The energy difference between a singlet ($\uparrow\downarrow$) state and a triplet ($\uparrow\uparrow$) state is affected by an external magnetic field. This energy difference is generally small for fields of the magnitude of the Earth's magnetic field. But the magnetism that living cells generate is even smaller. A magnetically sensitive reaction of this type is therefore not subject to significant thermal noise. However, a detection limit can be established by considering a model in which reacting product molecules can bind to receptors. There is an innate stochasticity in chemical reactions; rates represent an average behavior, and there is a Gaussian distribution around this average. This is called fundamental chemical noise, and we will come back to it later in this chapter. In this model, the average number of occupied receptors varies with the magnetic field, and the detection limits are set by this fundamental chemical noise [24]. The fact that many bird species actually need light for their magnetic compass to work is a strong indication that singlet–triplet transitions are involved in the navigation. Recently, additional evidence was found when it turned out that robins get disoriented when they are subjected to an RF magnetic field that oscillates at the singlet–triplet resonance frequency [5] (for more details, see Chapter 6 on free radical models).

The second mechanism that has been proposed to explain magnetosensitivity involves the small (<100 nm in diameter) granules of magnetite (Fe_3O_4). This material, also known as lodestone, is biochemically formed and has about 30% of the magnetic strength of pure Fe. In the 1970 s, it was discovered that certain microbes use single-domain magnetite granules, also called magnetosomes, as a kind of rudder to help them stay under water right at the interface between the water and the mud at the bottom. There is a force trying to align the magnetic granule(s) with the Earth's magnetic field,

and the microbe thus ''finds out'' what its own orientation is relative to the inclination of the Earth's magnetic field [25,26]. For a single-domain magnetite granule of about 100 nm in diameter, the product μB of the magnetic moment μ and the Earth's magnetic field B amounts to about $5kT$. This $5kT$ alignment is sufficient to exceed the kT thermal agitation in the granule's rotation. In higher animals it appears that the granules are commonly embedded in biopolymers and lined up to form a rigid linear rod. Such an alignment effectively increases the magnetic moment and thereby the sensitivity to small variations in the magnetic field [27]. Indications are that there can be up to a million magnetite-containing cells in the brain of almost any animal. Even humans, who exhibit no apparent magnetosensitivity, have magnetite in their brain tissue [7,8].

The intensity of the Earth's magnetic field varies from 25 to 65 μT, and the direction varies from parallel to perpendicular to the Earth's surface. The magnetic sensitivity of, for instance, homing pigeons has been shown to be such that field variations smaller than 10 nT can be detected. With such a sensitivity the pigeon can use the change of the magnetic field vector to furnish itself a kind of global positioning system (GPS) [29]. Recent data indicate that some birds incorporate both magnetite and singlet–triplet chemistry in their magnetosense [5].

It is tempting to hypothesize that extremely low-frequency (ELF) radiation or microwave radiation could have a physiological effect through the interactions with magnetosomes. Cells produce their own electricity and concurrent electric noise. But there is no significant endogenous magnetic field noise. So the magnetic part of ELF radiation or microwave radiation would not have to compete against such endogenous biological noise. The average 24-h personal 60-Hz magnetic field due to house wiring, distribution lines, electric motors, etc., for individuals in the U.S. population is about 10^{-7} T [30], that is, orders of magnitude smaller than the earth's stationary magnetic field. Starting from this premise, the magnetosome in the cytoplasm was modeled as a damped harmonic oscillator with an external 60-Hz modulation [31]. The restoring force is the force pushing to align the magnetosome's moment with the earth's magnetic field, and the damping is due to the viscosity of the cytoplasm. The associated equation is easily solved. Using reasonable values for the involved parameters, it is was found that even with exposure to a 60-Hz field with an amplitude of 5 μT, the alternating field transfers an amount of energy to the magnetosome that is orders of magnitude smaller than kT. In other words, the thermal agitations in the rotation far overwhelm any ''signal'' from an ambient 60-Hz field. But subsequently, the legitimacy of a simple linear approximation was questioned [32]. It was pointed out that there are intricacies that make the viscosity of the cytoplasm, which determines the damping coefficient in the model, hard to specify. Most importantly, the possibility of many individual magnetosomes in a cell acting in concert should be considered. With N magnetosomes in a cell instead of just one, the signal-to-noise ratio is $\sqrt{N}$ times larger. The explanation for this apparent amplification is the same as with the aforementioned N ion channels in the shark's electroreception. An alternative model that includes such cooperativity leads to a signal-to-noise ratio that is well over unity with a 2-μT amplitude 60-Hz magnetic field [32]. However, almost nothing is currently known about how forces on magnetosomes are transduced into physiological signals. More solid estimates of detection thresholds can probably be derived only after such biophysical mechanisms are revealed.

Electric fields are also of interest. Close to a power line, a human can be exposed to an electric field of about 10 kV/m. Two steps have to be taken to get to an assessment of the transmembrane voltage that such an exposure leads to. First of all, living tissue is much more conducting than air. So, charge in the tissue will move and follow the external field until it is compensated. Depending on the amount of movable dipoles, different materials

have different dielectric permittivities. The ratio between the internal field and the field in the air is [33,34]:

$$\frac{E_i}{E_0} \approx \varepsilon_0 \omega \rho_t \tag{7.4}$$

Here $\varepsilon_0 = 8.8 \times 10^{-12}\ \mathrm{C^2/(N\,m^2)}$ represents the dielectric permittivity of a vacuum, ω is the angular frequency ($2\pi f$), and ρ_t is the resistivity of the tissue. So for a frequency of about 100 Hz and with a typical tissue resistivity of about 1–2 Ω m, the attenuation factor for the field entering the body is found to be in a range of 10^{-8}–10^{-7}. Hence, most of the external field goes around the person in the way water in a river flows around a big rock. Once inside the tissue, an amplification at the cell membranes occurs again through the mechanism explained in the previous paragraph. For a spherical cell with a diameter of about $d = 10\,\mu\mathrm{m}$ in a field E, the voltage across the diameter will be $\Delta V = Ed$, and the eventual field in the membrane will be of the order of $E_{\mathrm{mem}} \approx E(d/h)$, where h is the thickness of the membrane. With $h \approx 5\,\mathrm{nm}$ we find an amplification factor of about a 1000. We thus find a net conversion factor of 10^{-5}–10^{-4} and an electric field of about 0.1–1.0 V/m across a membrane as a result of the 10-kV/m power line exposure. This leads to an ELF-induced potential difference of at most 10^{-8} V across the membrane. It should, however, be noted that muscle cells or nerve cells are cylindrically shaped and may have lengths in the millimeter or even centimeter range. When the imposed field is along the axis of the cylinder, there may be a conversion factor at the caps of the cylinder that is two to three orders of magnitude higher.

When a living cell is suddenly exposed to an external electric field, ions will start flowing in the conducting interior to compensate for this field. In a typical mammalian cell, it is generally within microseconds that ions have accumulated near the membrane to achieve a zero intracellular electric field. This means that stationary electric fields and ELF (<300 Hz) AC fields distribute over cell membranes. Power lines and high-voltage distribution stations have been the subject of a lot of public anxiety. The power grid operates at 60 Hz in the United States and at 50 Hz in most other countries, that is, well within the ELF regime.

The 10^{-8} V that we derived may appear small relative to, for instance, the transmembrane potential of about 0.1 V that is present in about every living cell. However, when we talk about detectability, this 10^{-8} V should first be compared to the transmembrane voltages due to Brownian motion. The thermal noise voltage across standard resistors was already detected in the 1920s [35]. A formula was subsequently derived by Nyquist [36]:

$$\langle dV^2 \rangle = 4kTRdf \tag{7.5}$$

This equation gives the average square voltage in a frequency window of width df. The noise is white, that is, it has the same intensity at all frequencies. Technically, this would lead to an absurdity. It would imply that the noise carries an infinite amount of energy. However, as Nyquist already pointed out, $\langle dV^2 \rangle$ starts vanishing when we get to high frequencies f where $hf \approx kT$. Here, h represents Planck's constant, $h = 6.6 \times 10^{-34}\,\mathrm{J\,sec}$. At these high frequencies, quantum physics takes over and makes $\langle dV^2 \rangle$ go to zero. Such high frequencies are not in our realm of interest.

What Nyquist had in mind for a resistor in his derivation was a Brownian gas of frequently colliding charge carriers. With a 5-nm cell membrane that consists of a lipid bilayer with embedded proteins, the charge carriers are small ions (Na^+, K^+, Cl^-, etc.).

The ions do not form a ''gas'' inside the membrane, and it is not *a priori* obvious that Nyquist's formalism would apply. The equilibrium noise current through a membrane that separates two ionic solutions is due to two-sided shot noise. Shot noise was first described by Schottky [37] in the context of vacuum amplifier tubes. It is due to the elementary charge being finite and the charge carriers making random ''jumps.'' It can be shown that two-sided shot noise ultimately leads back again to Nyquist's Equation 7.5 [38,39]. Ultimately, Equation 7.5 is a manifestation of something much more general than Nyquist may have had in mind. What underlies Equation 7.5 is Einstein's fluctuation–dissipation theorem. This theorem says that the same random collisions that cause diffusion, thermal noise, or shot noise also cause dissipation, friction, or resistance. The theorem, moreover, makes this connection quantitative:

$$\beta = \frac{kT}{D} \tag{7.6}$$

For the motion of a macromolecule in a liquid, D is the diffusion coefficient and β is the coefficient of friction, that is, the ratio $\beta = F/\upsilon$, where F represents the pulling force and υ represents the resulting average speed. But in the context of the current through a membrane, β represents the electrical resistance ($R = V/I$). For D we find $D = e^2 P_S c$ in the membrane electrical case. Here, P_S is the membrane permeability to the monovalent ion S that is responsible for the current, c represents the concentration of this ion on both sides of the membrane, and e is the elementary charge.

Electrically, a cell membrane can be modeled as in Figure 7.1a. A lipid bilayer membrane has a capacitance of about 1 $\mu F/cm^2$. The capacitance of an actual cell membrane is generally not much different. The resistance of a pure lipid bilayer depends on the ionic concentrations of the solutions on either side of the membrane. With these concentrations at biological levels the resistance of a lipid bilayer membrane can be as high as $10^9\ \Omega\,cm^2$. Because of the presence of ion channels, ion transporters, and ion pumps [40,41], an actual cell membrane has a resistance that is orders of magnitude smaller (typically about $10^3\ \Omega\ cm^2$). The resistance of a patch of membrane is inversely proportional to the area of that patch. So, in order to characterize a membrane, the approach is to measure the resistance through an actual patch and then multiply it with the surface area of that patch. That is why we give the resistance of a membrane in terms of $\Omega\ cm^2$.

The setup in Figure 7.1a is equivalent to the one in Figure 7.1b, that is, an ordinary RC circuit. When calculating the characteristic time, RC, of the circuit, the surface area cancels

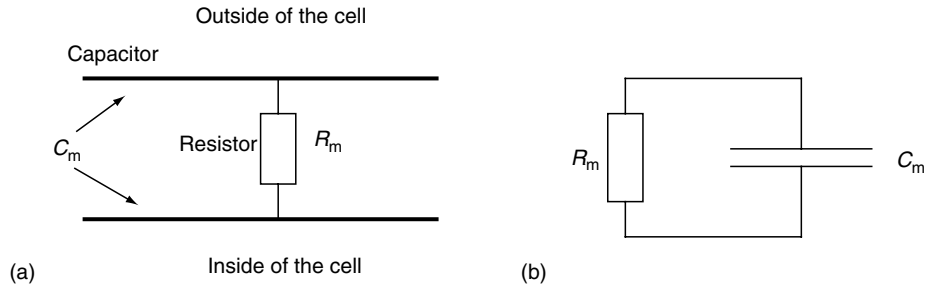

FIGURE 7.1
The electrical structure of the membrane is shown on the left. R_m and C_m are the resistance and capacitance between the inside and outside of the cell, respectively. The resistor also provides a thermal electromotive force. The equivalent circuit is shown on the right.

out. For a pure lipid bilayer the *RC* time constant can be of the order of minutes. But for a cell membrane it is of the order of milliseconds.

In our context, the resistor in Figure 7.1 is not just a resistor, but, following Nyquist (cf. Equation 7.5), also a white noise generator. At each frequency the resistor generates a harmonic oscillation. All these harmonic oscillations have the same amplitude. To evaluate the voltage across the capacitor, we thus have to analyze a simple *RC* circuit with an AC source. It has been argued that the high frequencies, that is, $f > (RC)^{-1}$, that are generated in the resistor do not have enough time to build up across the capacitor [42]. However, for low-frequencies, that is, $f < (RC)^{-1}$, changes are sufficiently slow for the capacitor to keep up and follow the voltage in the resistor. In this view the transmembrane voltage is the voltage across the capacitor, and the equilibrium noise is thus expected to occur mostly at low-frequencies. As mentioned before, the *RC* time of a cell membrane is of the order of milliseconds, and ELF fields thus operate in the $f < (RC)^{-1}$ regime where the noise is largest. A straightforward quantitative analysis shows that the low-frequency equilibrium noise far overwhelms any reasonable ambient power frequency field [42]. There would be no way to ever instantaneously detect such a field.

It was later put forward that everything that is happening in the cell membrane should, in the model of Figure 7.1, be imagined to happen inside the resistor [43]. Membrane proteins go through their catalytic cycle against a background of intramembrane noise. Inside the membrane means, in the context of Figure 7.1, inside the resistor. In this picture, the thermal noise voltage (cf. Equation 7.5) derives from a net electric field that results from inhomogeneities in the distribution of the charge carriers. Now at low-frequencies, the capacitor will be able to follow the imposed oscillation and effectively produce a field to counter the field generated inside the resistor (Figure 7.1a). This model thus leads to a vanishing net potential inside the membrane at low-frequency. At high frequency, the voltage changes in the resistor are too fast for the capacitor to keep up with. The capacitor will remain uncharged, and the thermal AC voltage will not be compensated for.

However, Figure 7.1 is no longer the appropriate model when we try to derive the intramembrane electric fields. For a cell of about 20 μm in diameter, the surface area amounts to about a billion square nanometers. The membrane is only about 5 nm thick, so the resistor resembles a very thin sheet. The lateral conductivity, that is, the conductivity from one place on the sheet to another, is very low. So at different spots on the sheet, different unrelated noise fields are generated. The more sensible model would therefore be one where the resistor in Figure 7.1 is cut up into millions of independent parallel resistors. Each of these resistors creates its own field. The capacitor plate corresponds to the conducting liquid on either side of the membrane, and it can be conceived of as having perfect lateral conductivity. So each resistor generates its own particular field, but they all experience the same field from the capacitor. With this model the noise gets very large. Not only there are more, say *N*, resistors producing noise. Each of these resistors has a resistance *NR* (*N* parallel resistors of resistance *NR* lead to a net resistance of *R*) and, according to Equation 7.5, thus produces more noise. Because the *N* parallel resistors that make up the resistance *R* are independent, they oscillate out of phase at each frequency *f*. As a result the parallel resistors end up pushing a lot of current in and out of each other. Most of the generated noise current thus remains intramembrane and never reaches the capacitor. The mathematics associated with this parallel setup is challenging, but an exact solution can be derived [39,44]. The capacitor, and therefore the *RC* time, plays no role in the intramembrane noise. The intramembrane noise is white and has an intensity that is many orders of magnitude larger than the noise that reaches the capacitor. What matters for biological function is actually the intramembrane noise. This, after all, is the noise that a membrane-embedded protein would ''feel.'' The protein's catalytic cycle takes place

against the background of such noise. The parallel setup model leads to a noise intensity that is much larger than that of the earlier models.

At first sight, all this extensive treatment of intramembrane noise may seem to have little to do with the two-sided shot noise that a membrane is subject to. However, when rigorously modeling the membrane as a thin sheet in an ionic solution, something similar to the overwhelming intramembrane noise is found. The ions that constitute the net charge on the membrane in Figure 7.1a move across the membrane–solution interface with an average speed of about 100 m/sec. This is just their thermal motion, and it is easily derived from $(1/2)mv^2 \approx kT$. This effectively causes laterally traveling electric pulses in the membrane. The noise intensity of these traveling electric pulses appears to be many orders of magnitude higher than the noise that is due to the shot noise-like membrane passages by the ions [39].

Current models of membrane noise thus lead to transmembrane voltage noise estimates that far exceed the strength of any reasonable magnitude ELF field-induced ''signal.'' What the previous paragraphs lead up to is the conclusion that an ELF signal cannot be detected instantaneously.

However, under certain conditions and given enough time, even the smallest signal can get out of the noise band. The following example is meant to illustrate this. Consider the system depicted in Figure 7.2. Let the the resistance R represent a membrane patch. For simplicity, imagine that on either side of the resistor there is an infinite reservoir (i.e., a capacitor with infinite capacitance), so no net voltage can develop across the resistor. The average square charge $\langle q^2(t)\rangle$ that accumulates on either side of the membrane can be easily derived from Equation 7.5 and amounts to

$$\langle q^2(t)\rangle = \frac{2kT}{R}t \tag{7.7}$$

Again, there is an obvious analogy between Equation 7.7 and the well-known diffusion formula $\langle x^2(t)\rangle = 2Dt$, which describes the average square displacement of a particle with a diffusion coefficient D during a time interval of length t. The above formula clearly shows how, in an electrical context, kT/R plays the role of the diffusion coefficient D.

From Equation 7.7 we infer that for the accumulated charge as a function of time we have $|q_{\mathrm{Br}}(t)| \approx \sqrt{\langle q^2(t)\rangle} \propto \sqrt{t}$. The thermal noise-driven accumulation of any charged or uncharged molecule on either side of the membrane carries this $\sqrt{t}$ proportionality. The coupling of ELF electromagnetic fields to biochemical activity occurs mostly through

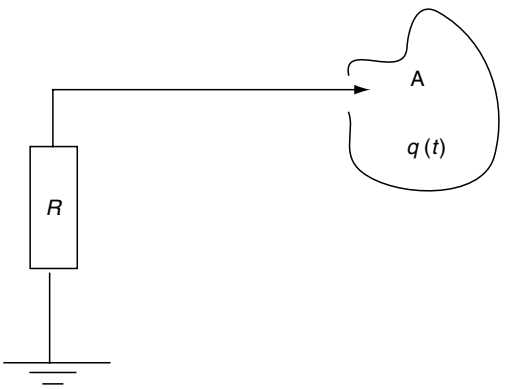

FIGURE 7.2
A resistor is connected to the ground and to an infinite reservoir A. The net voltage between the reservoirs remains zero. The situation is like the one in Figure 7.1 with the capacitor having infinite capacitance. Because of Brownian motion of electrons in the conduction band, there is a zero-average fluctuating current through the resistor. The net charge accumulating in the reservoir A is the result of these fluctuations in the same way that diffusive displacement is the result of random Brownian kicks. We have $\langle q^2(t)\rangle = 2(kT/R)t$ for the average square charge accumulation in time t.

membrane proteins. Membrane proteins whose conformational changes involve significant changes of the dipole moment are particularly sensitive. ELF fields can affect the catalytic rates of such proteins. So, for instance, electrogenic ion pumps [41], and also transporters or pumps that just carry a dipole, may have a slightly altered throughput in the presence of an ELF field. If there is no restoring force for a transported or pumped molecule, the accumulation will continue. The cumulative effect of the altered throughput will be a linear function of time. The excess charge that accumulates because of an ELF field thus follows $q_{\mathrm{ELF}} \propto t$.

Consequently, we see that on a small timescale the Brownian noise ($\propto \sqrt{t}$) will be stronger than the signal ($\propto t$). But there will always come a time $t = t_*$ when $|q_{\mathrm{B}r}(t_*)| = |q_{\mathrm{ELF}}(t_*)|$, and we then achieve S/N = 1. It depends on the values of the proportionality constants when t_* occurs. If molecular change is the measurement criterion, then it is only on timescales of the order of t_* that the effect becomes measurable. Estimates for t_* with realistic ELF exposure have been made [45] and have led to a timescale larger than the age of the universe.

7.6 Nonequilibrium Noise

In the previous section, we considered equilibrium noise. A living cell, however, constitutes a system that is far from equilibrium. Between the intracellular and extracellular solutions there is an electric potential difference of about 100 mV. For ions like Na^+, K^+, Cl^-, and Ca^{2+} there is a more than tenfold difference between intra- and extracellular concentration. The 100-mV transmembrane voltage over a width of about 5 nm implies a very strong field of tens of megavolts per meter.

The electrochemical potential across the cell membrane is an energy source for many processes [41]. The Na, Ca exchanger, for instance, is a membrane protein that picks up a sodium ion on the outside and then goes through a cycle in the course of which it drops the sodium ion off on the inside. The protein couples the energetically downhill movement of sodium to the uphill transport of calcium. In the course of the cycle a calcium ion is picked up on the inside and pumped, against the electrochemical potential, to the outside. The membrane potential is maintained by ATP-driven ion pumps. The most common of these is Na, K-ATPase. This is a membrane protein that, in the course of its catalytic cycle, hydrolyzes one ATP and uses the released energy to transport three sodium ions out of the cell and bring two potassium ions in.

Each working protein is like a small engine. A living cell contains millions of these engines: they are continuously converting energy from one form to another, and in the process, they are also generating heat, that is, dissipating energy. A living cell constitutes a far from equilibrium system, and the continuous transduction and dissipation of energy generates noise, which adds to the thermal, Brownian noise that was discussed in the previous section.

It would not be against the first law of thermodynamics (i.e., conservation of energy) if ion pumps were to extract heat from the environment and use it to power the maintenance of the transmembrane potential. This would, however, be in gross violation of the second law of thermodynamics. There are many equivalent formulations of the second law. The most common formulation is the proposition that every isolated system strives to increase and maximize its entropy. The teleological form of this formulation is somewhat bewildering. After all, most laws in science are formulated as conservation laws, for

example, conservation of energy, or as causal laws, for instance, Newton's $F = ma$. However, after properly defining entropy, entropy maximization is often the easiest form of the second law to work with when dealing with macroscopic systems.

When going to the molecular realm, the second law can pose some challenging paradoxes. Consider, for instance, an ion channel in a cell membrane. Many ion channels rectify, that is, they pass current more easily in one direction than in the other. So the I–V characteristic is not a straight line through the origin, but it also has a curvature. Any frequency from the white spectrum of equilibrium noise should, in principle, be rectified. It thus might look like a rectifying ion channel could use zero-average equilibrium Nyquist noise to charge a battery. It would not work, of course. As pointed out above, it would be in violation of the second law. Thinking in the context of rectifying p–n junctions, solid-state physicists ran into this paradox long before ion channels were discovered. In 1950, L. Brillouin wrote a paper ''Can the Rectifier Become a Thermodynamic Demon?'' [46]. In this paper, he presents a short derivation to show that in a circuit with all components at the same temperature, no diode can rectify. He is aware that his case represents a special case of the so-called principle of detailed balance: ''No system in thermal equilibrium in an environment at constant temperature spontaneously and of itself arrives in such a condition that any of the processes taking place in the system by which energy may be extracted, run in a preferred direction, without a compensating reverse process.'' The principle is a consequence of the second law [47,48] and, for our rectifier, basically states that there must, on average, be as much current in one direction as there is in the opposite direction.

In the *Feynman Lectures on Physics* [49] a ratchet and pawl system, originally thought up by Smoluchowski [50], is considered and eloquently discussed. The device operates as a mechanical rectifier (Figure 7.3) and essentially establishes the mechanical equivalent of Brillouin's paradox. The paradox is solved with the realization that the pawl must also be

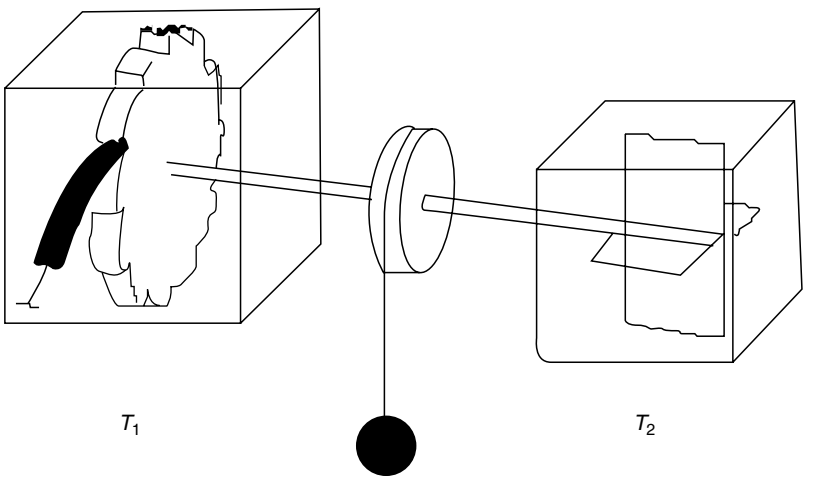

FIGURE 7.3
The mechanical thermal ratchet as it was originally conceived by Smoluchowski [50] and later discussed by Feynman et al. [49]. The device is small, and the paddle wheel in the right reservoir is moved by collisions of the molecules from the surrounding medium against the paddles. Because of the asymmetry of the teeth, the ratchet and pawl in the left reservoir allow motion in one direction and block it in the opposite direction. With the resulting net rotation it should be possible, in principle, to lift a weight. However, it would be in violation of the second law of thermodynamics to extract work from thermal fluctuations in the equilibrium situation, that is, $T_1 = T_2$. The solution of the paradox lies in the realization that the ratchet and pawl are also subject to thermal fluctuations if the system is small.

subject to thermal noise. The pawl involves a spring, and the spring will, at thermal equilibrium, exhibit a Boltzmann distribution over the accessible energy range. Even here the second law is involved, though on a deeper level. Given the macroscopic variables (e.g., temperature, concentration, pressure, etc.) there are still many possible molecular arrangements, that is, microstates, that correspond to that macrostate. For a fixed amount of energy the Boltzmann distribution is the energy distribution that has the most permutations [20]. It is therefore the most likely distribution. On the level of statistical mechanics, the second law can be formulated as the rule that given a macrostate, every microstate that corresponds to that macrostate has equal probability.

Second law issues can be subtle. The connection between statistics, entropy, information, and physical work still poses paradoxes that are hard to fathom. Books and articles still appear in which researchers are attempting to come to a fuller understanding and a better intuition [51,52]. At the scale of ion channels the simple invocation of detailed balance reveals little. An appropriate description is like the one Feynman gave for his mechanical ratchet and pawl: it involves Boltzmann distributions and Brownian motion. So it would simply be wrong to take any frequency from the white spectrum of equilibrium noise and model a rectifying ion channel as subject to this oscillation. The ion channel itself and its Brownian fluctuations have to be included in the description. At equilibrium, no part of a system can be ''subject'' to any other part. This is what detailed balance can be interpreted to mean.

However, when energy is dissipated, it is possible for one part of the system to impose its fluctuations on another part. When a rectifying ion channel is subject to nonequilibrium fluctuations, it will actually rectify the fluctuations and drive a net current. Consider, for instance, an electrogenic ion pump like Na,K-ATPase. As was mentioned before, this pump utilizes the energy of ATP hydrolysis to pump three sodium ions out and pump two potassium ions in. All this transport is against the electrochemical potential and requires about $15kT$ units of energy per stroke under physiological conditions. The power source is the hydrolysis of ATP, which under physiological conditions, releases about $20kT$ units of energy per cycle. It is the remaining $5kT$ that drives the process forward and that is ultimately released as heat. Na,K-ATPase is binding and releasing ions and thus generates fluctuating electric fields in its direct vicinity. For a nearby ion channel these fields can be conceived of as imposed because the $5kT$ that drives the Na,K-ATPase cycle is enough to overwhelm the small amount of energy ($<1kT$ [53]) necessary for the opening or closing of a channel. There is no feedback from the channel to the pump. The channel will rectify the fluctuations as a result, and a zero-average field can thus lead to net charge transport. In essence, the nonequilibrium fluctuations generated by the pump and imposed on the channel are part of the conversion of chemical energy, that is, the energy in ATP, to an electrochemical potential across the membrane.

So energy-dissipating, nonequilibrium oscillations and fluctuations are able to do work. ELF radiation from outside the organism can impose a varying field on an ion channel in much the same way that the nearby ion pump from the previous paragraph can impose a field on an ion channel. ELF radiation brings energy into the organism. Part of this energy will be dissipated to become heat, and part of it may be converted into chemical or electrical work. There is obviously no feedback from an ion channel back to the ELF source.

The selectivity of ion channels for the different kinds of ions is still hard to understand and model. But the rectification property is much easier to intuit (Figure 7.4). The channel is shaped like an asymmetric double cone, and charges in the lining of the channel are

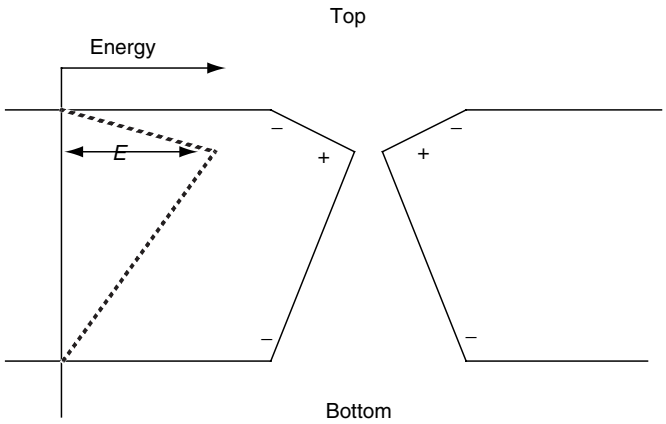

FIGURE 7.4
A simple continuum model of an ion channel imagined to be shaped like an asymmetric double cone. The energy profile on the left depicts the activation barrier that a positive ion going through the channel has to pass. The barrier has an obvious anisotropy.

indicated in the figure. A sodium or potassium ion that is going from the top to the bottom of the channel faces a rapid increase of the potential and then a slow decrease. A sodium or potassium ion that goes through in the opposite direction faces a slow increase and a fast subsequent decrease. A positive ion thus has a larger force to overcome when going from top to bottom than when going from bottom to top. Because of this, an imposed zero-average oscillation will lead to a net current [54]. As a matter of fact, any anisotropic potential shape along the length of the channel will rectify a zero-average harmonic field to lead to a net current [55]. Ion channels are proteins consisting of many amino acids, and anisotropy along the inside lining will be the rule rather than the exception.

The plethora of ratchet research in the late 1990s has made it clear that almost any zero-average oscillation or fluctuation imposed on a ratchet-like structure as in Figure 7.4 leads to a net current. Imagine, for instance, a temperature oscillation. With energy expressed in units of kT, a variation in temperature implies an oscillation of the barrier height E. Because of the difference in relaxation times on the slopes on either side of the barrier, a net current will result [55–58]. Recently, ever more examples have been found of nature exploiting ratchet effects for the purpose of regulation [59].

Researchers have meanwhile also succeeded in making artificial channels. Cone-shaped (and therefore anisotropic) channels form when a heavy ion is shot through an artificial membrane [60,61]. The I–V characteristic for the current of different types of ions has subsequently been recorded. It has even been experimentally shown that net charge transfer results when a zero-average field is imposed on such an artificial channel. The channel is thus made to behave like a kind of pump that converts an AC input into a DC output [62].

Imagine a number of identical anisotropic channels in a vesicle with an otherwise impermeable membrane. Next, put a large number of such vesicles in a beaker with an ionic solution. Any nonequilibrium fluctuation from the environment, or any ''signal'' for that matter, will now be picked up and converted into an electrochemical potential. The convection caused by a temperature gradient will heat up and cool down the vesicles and lead to their electrically charging up. The electric component of an ELF electromagnetic field will do the same thing. The beaker could thus be a battery that recharges by harnessing any incoming nonequilibrium fluctuation. This mechanism might, moreover, have played a role in the emergence of early prokaryotic life.

The Fourier spectrum of the noise that is associated with processes that dissipate energy is not white. Nonequilibrium noise appears to have higher amplitudes at lower frequencies; in other words, it exhibits an intensity that decreases with frequency. The so-called $1/f$ noise was first studied in the 1920s in the very nonequilibrium context of thermionic vacuum tube amplifiers [37]. In current scientific discourse the term ''$1/f$ noise'' actually applies to all noises that have spectral densities behaving like $1/f^{\alpha}$, where α ranges from about 0.5 to about 1.5. Especially in electrical devices, such noise is very commonly and easily observed. It is also known as ''excess noise'' or ''flicker noise.'' In a log–log plot the $1/f^{\alpha}$ behavior usually extends over several frequency decades.

In the 1930s, it was proposed that the flicker noise originated from a variable number of electrons present in the conduction band. Electrons would shuttle between a free state and a bound state as in a chemical reaction. Let the relaxation time of that reaction be $1/\lambda$. This leads to a simple exponential relaxation $N(t) = N_0 \exp[-\lambda t]$ after any kind of fluctuation that has a magnitude N_0. The Fourier transform of the exponential decay is easily found:

$$F(\omega) = N_0 \int_{t=0}^{\infty} \exp\left[-(\lambda + \mathrm{i}\omega)t\right] \mathrm{d}t = \frac{N_0}{\lambda + \mathrm{i}\omega} \tag{7.8}$$

For the power spectral density, $S(\omega) = \|F(\omega)\|^2$, we find:

$$S(\omega) \propto \frac{1}{\lambda^2 + \omega^2} \tag{7.9}$$

where the proportionality constant involves the magnitudes of the fluctuations as well as the rates at which fluctuations occur. The power spectral density is a useful quantity as it describes how the energy in the noise is distributed over the different frequencies. $S(\omega)\mathrm{d}\omega$ is proportional to the amount of power that the noise carries between the frequencies ω and $\omega + \mathrm{d}\omega$. Equation 7.8 describes a so-called Lorentzian power spectrum. With a log scale for the frequency, the resulting curve is a sigmoid. At high ω, $S(\omega)$ behaves like $1/\omega^2$. As better data became available, it was found that a better fit was obtained when a distribution of infinitely many relaxation times was assumed [63]. Take, for instance, a uniform distribution of relaxation times between λ_1 and λ_2. With Equation 7.9 this leads to:

$$S(\omega) \propto \frac{1}{\lambda_2 - \lambda_1} \int_{\lambda_1}^{\lambda_2} \frac{1}{\lambda^2 + \omega^2} \mathrm{d}\lambda = \frac{1}{\omega(\lambda_2 - \lambda_1)} \left\{ \arctan\frac{\lambda_2}{\omega} - \arctan\frac{\lambda_1}{\omega} \right\} \tag{7.10}$$

It is easy to check that on $\lambda_1 < \omega < \lambda_2$ this $S(\omega)$ is approximately proportional to $1/(\omega(\lambda_2 - \lambda_1))$. This $S(\omega)$ is, moreover, roughly constant for $\omega < \lambda_1$ and drops off like $1/\omega^2$ when $\omega > \lambda_2$.

If we let, between λ_1 and λ_2, the relaxation rates contribute proportional to $\lambda^{-\beta}$, we can actually get any $1/f^{\alpha}$ dependence that we want, since

$$S(\omega) \propto \int_{\lambda_1}^{\lambda_2} \frac{1}{\lambda^{\beta}(\lambda^2 + \omega^2)} \mathrm{d}\lambda \propto \frac{1}{\omega^{1+\beta}} \quad \text{for } \lambda_1 < \omega < \lambda_2 \tag{7.11}$$

At $\omega < \lambda_1$, this spectrum would again flatten out.

In experimental practice with electrical resistors and amplifiers the $1/f^{\alpha}$ behavior has been observed to extend over more than six frequency decades with no noticeable flattening at low-frequency [64].

$1/f^{\alpha}$ spectra have been observed in nature in a wide variety of systems: electrocardiac waves [65], the variation of sea levels [66], tardiness at work [67], etc. An essential feature of $1/f^{\alpha}$ noise is that it exhibits self similarity, that is, if one magnifies both time and space with the appropriate factor, the noise pattern is indistinguishable from the original one. So the noise does not have a characteristic timescale or length scale. $1/f$ noise is often seen as a signature of the fractal character of nature.

In 1987, Bak et al. [68] proposed a model for a universal mechanism behind $1/f$ noise. In their landmark paper they illustrated the concept of ''self-organized criticality'' with a sandpile model. When a sandpile has an inclination steeper than a critical angle θ, avalanches will occur that bring the pile back to the critical angle. When sand is added to the pile in a random fashion, these avalanches do not exhibit a characteristic size, nor do they appear after regular time intervals. Instead, there are bigger avalanches that are relatively rare and smaller avalanches that occur more frequently. The size distribution follows a power law in the frequency f. For instance, in one day there can be one avalanche involving more than 1000 grains, 10 involving more than 100 grains, 100 avalanches involving more than 10 grains, and so on. The picture that emerges is one of a system that is sitting on the critical edge between two phases and is ''organizing'' avalanches to stay there [69]. The most commonly cited real-life example of self-organized criticality is the Gutenberg–Richter power law for earthquakes. It appears that every year, on average, there is one earthquake larger than magnitude 8, 10 earthquakes larger than magnitude 7, and 100 earthquakes larger than magnitude 6. Self-organized criticality is an attractive theory. It proposes a simple mechanism and predicts power laws that can be easily verified or falsified. It has been utilized in a wide variety of contexts [69]. It has, for instance, been applied to evolutionary theory [70] and has been used to explain frequency-size distributions of forest fires [71].

How truly universally applicable self-organized criticality is and to what extent its claims may be unwarranted are matters that are still very much under debate. The $1/f$ proportionality for earthquakes applies only between magnitudes 5 and 8. Even for the archetypal sandpile, things turn out to be more involved upon close inspection than self-organized criticality suggests. Accurate measurements [72–74] on real sandpiles showed that in many cases there is no $1/f$ pattern in the avalanches. It turns out that system parameters, like the grain size and the rate of sand addition, determine to a large extent what kind of spectrum eventually emerges. The entire concept of self-organized criticality collapses, of course, if fine tuning by the experimentalist is crucial for the $1/f$ spectrum to materialize. All in all, $1/f$ noise is not as universal as first thought, and the dynamics behind nonequilibrium noise are usually best unraveled with *ad hoc* models.

The node of Ranvier is where the action potential for myelinated nerve cells is generated [75]. There is a high concentration of ion channels in the node of Ranvier, and in the days before patch clamp, it was a good place to record membrane electrical activity. In the mid-1960s, Verveen and Derksen measured 5–10 min of cell membrane voltage noise at a Ranvier node of an unstimulated nerve cell [76,77]. The resulting power spectrum showed two decades, between 10 Hz and 1000 Hz, of $1/f$ noise (see Figure 7.5). This $1/f$ noise, they found, was much larger in magnitude than what Nyquist's $4kTR$ formula (cf. Equation 7.5) would predict. Following the explanation for $1/f$ noise in ordinary resistors (cf. Equation 7.10 and Equation 7.11), Verveen and Derksen suggested that an ion channel could, from time to time, get ''clogged up.'' The wide distribution of waiting times (i.e., the λs in Equation 7.8 through Equation 7.11) before getting unclogged would then give rise to the $1/f$ spectrum [78].

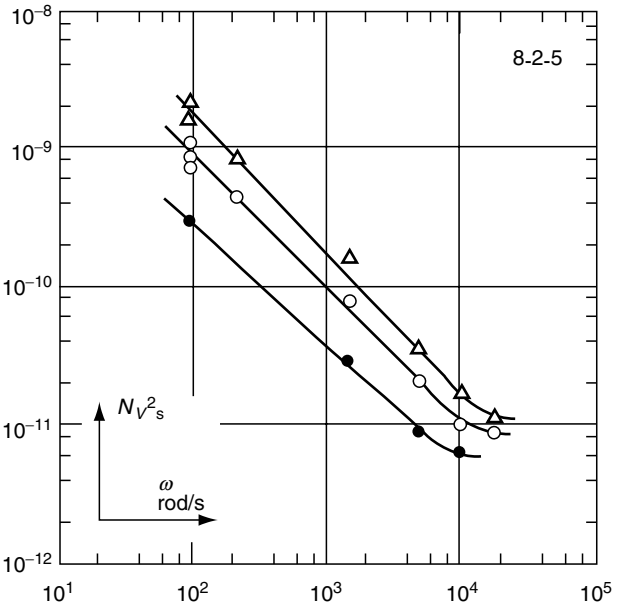

FIGURE 7.5
The voltage noise spectral densities from the frog node of Ranvier at room temperature at rest (open circles), at 10-mV depolarization (open triangles), and at 10-mV hyperpolarization (filled circles) [76,77]. (© Dutch Physiological Society. With permission.)

In the last two decades, single-channel recordings have shown how, even without stimulus, ion channels open and close repeatedly [40,75]. The kinetics behind the openings and closings is still very much a matter of debate. Modeling an ion channel as a two-state molecule with an open and a closed state and chemical steps with constant rates connecting these states appears not to account for the data in many cases. Electrophysiologists have commonly resorted to explaining the nonexponential distributions of open and closed times with a kinetic scheme that contains more than two states. With such an approach any distribution of open and closed times can always be fitted with a kinetic scheme [79–81]. It is just a matter of coming up with sufficiently many parameters (i.e., states and rates) to fit the data. In chemical kinetics the transitions are always assumed to be Markov transitions, that is, the probability of moving from a state 1 to a state 2 is constant and does not depend on the time that the molecule has been in state 1. A channel that is making such Markov transitions between a finite number of states always exhibits a power density spectrum that is a sum of Lorentzians. The number of characteristic times in the spectrum will always be one less than the number of states. If the characteristic times are sufficiently far apart, the power density spectrum will exhibit a number of identifiable plateaus when plotted on the customary logarithmic scale. The inflection points between the plateaus occur at the inverses of the characteristic times.

An alternative approach, foreshadowed by the aforementioned suggestion of Verveen and Derksen, has been to model the open to closed transition rates of an ion channel as time dependent, for instance $k(t) \propto t^{-\mu}$, where $0 < \mu < 1$ [82–85]. The exponent μ is taken to be smaller than unity to make $\int_{\tau}^{\infty} k(t)\, dt$ diverge for all $\tau > 0$ and thus guarantee the inevitability of an eventual transition. The proportionality $k(t) \propto t^{-\mu}$ leads to a decreasing transition probability, that is, the channel is ''stabilizing in its openess,'' as more time is spent in the open state. There is ample justification for the use of open–closed transition rates that vary in time. A protein has many degrees of freedom and is subject to many equilibrium and nonequilibrium fluctuations. If an intramolecular rearrangement, like a transition between an open and a closed state, can be modeled as the crossing of an

activation barrier, then that barrier will most likely not be fixed and stationary. A fluctuating barrier implies fluctuating open–closed transition rates. We could thus get the infinitely many relaxation rates that give rise to the $1/f$ power density spectra of Equation 7.10 and Equation 7.11. Under physiological conditions an ion channel is trafficking ions in an electric field of tens of megavolts per meter and comparable chemical gradients. This is a very nonequilibrium setup, and it has been conjectured that the channel operates as a self-organized critical structure. One authoritative textbook [65] states it as follows:

> A channel protein may be a self-organizing critical system. The channel protein consists of many pieces that interact with their neighbors. The energy added to the protein from the environment causes local strains that are spread throughout the structure. If these distortions spread faster than the time it takes for the structure to thermally relax, then the channel protein may be a self organizing critical system. If that is the case, then the fluctuations in the channel structure will be due to a global organization of the local interactions between many small interacting pieces of the channel protein. The fractal scaling would then be due to the fact the channel structure is poised at a phase transition between its open and closed conformational shapes.

Over the past few years increasing amounts of data have been gathered with ever more accurate technology. Recently, the $1/f$ power spectral density of a nerve cell that Verveen and Derksen discovered was more accurately rerecorded [86]. But through careful subsequent experimentation and computer simulations, these researchers were also able to show how the apparent $1/f$ result comes about as the sum of a number of Lorentzian contributions. Each type of channel has its own Lorentzian, and because of close characteristic times the sum of the individual sigmoids appears like a smoothly decreasing $1/f$ curve.

For a single channel, things often turn out to be much more intricate than simple $1/f$ versus Markov kinetics. In single-channel recordings of a bacterial ion channel it was found that actual channel openings and closings follow Markov kinetics and lead to Lorentzian contributions to the ultimate net power spectrum [87]. The $1/f$ noise that is present in the power spectrum originates from transitions between open states of a slightly different (about 1–5%) conductance. The rates of these miniconductance transitions appeared to be independent of the transmembrane voltage. The small transitions in conductance have been conjectured to be due to small clusters within the channel's structure moving in and out of the lining of the pore [87]. A cluster can cause a partial flow constriction when it sticks out into the pore. Following this idea, the apparent $1/f$ behavior can be attributed to many different clusters moving in and out with equally many different relaxation times. The voltage independence comes about because these clusters are either uncharged or the external electric field is somehow screened. Noise in synthetic channels has also been studied [88]. There it was found that potassium currents through a one-state, permanently open channel exhibit $1/f^2$ noise. An artificial channel that can open and close, on the other hand, was found to exhibit $1/f$ noise when the externally applied voltage is in the right regime. With this latter artificial channel there is good ground to attribute the open–closed transitions to the movement of ''dangling ends'' of polymers in the pore's lining. So the result supports the ''moving cluster'' for the mechanism behind $1/f$ noise in channels.

There appears to be no simple theory that can convincingly bring all manifestations of $1/f$ noise under one common denominator. All the indications are that an *ad hoc* approach to nonequilibrium noise phenomena is still the most fruitful one.

In ordinary resistors the amount of $1/f$ noise grows linearly with the dissipated power W. If we take $S(\omega)\,\mathrm{d}\omega$ to denote the power in energy per unit of time (watts) in an interval $\mathrm{d}\omega$, then we have for the power spectral density:

$$S(\omega) = \frac{gW}{f} \tag{7.12}$$

Here, g is a dimensionless constant the value of which depends on the type of resistor.

Nyquist noise is simple in that the net value of the resistance R fully determines the noise amplitude. With $1/f$ noise a more complex situation arises. Experimentally, the constant g (cf. Equation 7.12) turns out to be proportional to the volume-to-power ratio [89]. In Figure 7.6 the four resistors in design (b) are identical to the one resistor in design (a). It is obvious that (a) and (b) will have the same net resistance and therefore the same amount of Nyquist noise. Design (a), however, will exhibit four times as much $1/f$ noise as design (b). Design (b) is quieter because the energy dissipation is distributed over a larger volume. Generally, we have $g \propto 1/V$, where V denotes the resistor's volume. The gW in Equation 7.12 can be expressed as $g_\mathrm{e}w$, where g_e is the g-value for a single elementary charge carrier in the resistor and w is the energy dissipated in the volume of such a single, independent charge carrier.

Pumps and carriers move ions one by one. Imagine a single pump or carrier that moves ions across the membrane at a rate ν. During a small time interval $\mathrm{d}t$ there is a probability $p = \nu\,\mathrm{d}t$ that an ion is transported. We take $\mathrm{d}t$ to be sufficiently small so that the probability of more than one ion being transported during $\mathrm{d}t$ is negligible. We also take the duration of the catalytic cycle, that is, the ''processing'' time for an ion going through the membrane, to be negligible in comparison to the time between catalytic cycles. If we were not to make the latter assumption, we would simply have to multiply by the probability that an average channel is available for transport when we want to express the transport rate. For the average number of ions $\langle n\rangle_{\mathrm{d}t}$ transported by the channel in time $\mathrm{d}t$, we now have $\langle n\rangle_{\mathrm{d}t} = 1 \cdot p + 0 \cdot (1-p) = p$. For the variance we have $\sigma_{\mathrm{d}t} = \langle n^2\rangle - \langle n\rangle^2 = 1^2 \cdot p - (1 \cdot p)^2 = p(1-p)$. For M subsequent timesteps and $M\,\mathrm{d}t = T$, the variances add up, and we have $\langle n\rangle_T = Mp$ and $\sigma_T = Mp(1-p)$. So the standard deviation, $\sqrt{\sigma_T}$, works out to be proportional to $\sqrt{M}$. Over time the standard deviation becomes more and more negligible compared to the average. For sufficiently small $\mathrm{d}t$ we can take $1-p$ to be equal to 1, and we then have a variance that equals the average.

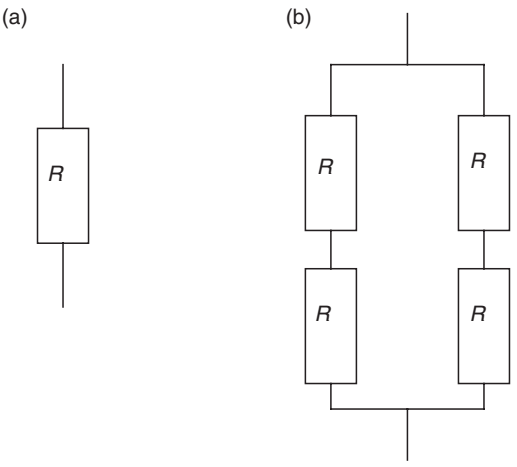

FIGURE 7.6
Design (a) and design (b) both have a net resistance R. They are different in that design (b) actually consists of two parallel resistors of $2R$. Designs (a) and (b) will exhibit the same amount of equilibrium noise, as it is only the net resistance (cf. Equation 7.5) that determines the equilibrium noise amplitude. It appears, however, that design (a) has four times as much power spectral density as design (b). The amount of nonequilibrium noise is proportional to the current density.

In the textbook by DeFelice [89] it is shown how the power spectral density of the process above amounts to $S(f) = 2\sigma_T/T = 2\nu$. The frequency-independent power spectrum can be intuited as follows. If the actual transport time through the membrane is small, then we can conceive of the transmembrane current as delta function-like pulses occurring at a rate ν. The Fourier transform of a Dirac delta function is a flat spectrum. In order to go from particle current to electrical current we must, to obtain the current power spectral density, multiply with the square of the charge of the involved ion. Taking this to be the elementary charge e, we find

$$S_i(f) = 2\nu e^2 = 2e\langle i\rangle \tag{7.13}$$

Here, $\langle i\rangle = e\nu$ denotes the average current through one pump.

Next, we let $\langle I\rangle$ denote the total transmembrane current due to pumps of a particular ion through the entire cell surface. We then have for the total current power spectral density:

$$S_I^{\mathrm{pu}}(f) = 2e\langle I\rangle \tag{7.14}$$

For a living cell in a steady state, for each kind of ion, there are just as many ions going in as there are going out, that is, there is just as much uphill transport through pumps as there is downhill flow through ion channels. So we have the same current $\langle I\rangle$ uphill as well as downhill. Below, we will first show that the downhill flow through the channels generates much more nonequilibrium noise than the uphill flow through the pumps. We will then show how the channel noise far exceeds the Johnson–Nyquist equilibrium noise.

Ion channels stay open for an average time of about $\tau_{\mathrm{op}} = 10^{-3}$ sec, and during that time there is a current of about 10^7 ions per sec (i.e., about 1 pA). So the equivalent of the elementary charge mentioned in the previous paragraph is now $N = 10^4$ ions.

However, before we blindly substitute Ne for e in Equation 7.14 to obtain the current power spectral density generated by the channel population of a cell, we have to take another source of variance into account. The channel-open time of about a millisecond is an average. If we view opening and closing of a channel as simple chemical steps between an open and a closed state, then the millisecond is the average of an exponential distribution of open times. For an exponential distribution the average open time equals the standard deviation in the open time. So the standard deviation ΔN equals N itself. The associated variance has to be added in. So we have $S_I^{\mathrm{ch}}(f) \approx 2\,\nu e^2\,(N^2 + (\Delta N)^2)$. The rate ν now represents the number of channel openings per unit of time. So we get for the current power spectral density produced by the channels:

$$S_I^{\mathrm{ch}} \approx 4Ne\langle I\rangle \tag{7.15}$$

So the channel contribution to the total nonequilibrium current noise is about 10^4 times as large as the contribution of the pumps. For the total current power spectral density, S_I^{noneq}, due to nonequilibrium currents, we thus neglect the pump contribution.

The above Equation 7.15 constitutes $S_I^{\mathrm{ch}}(0)$. At higher frequencies, when f approaches the average open time τ_{op} of the channel, $S_I^{\mathrm{ch}}(f)$ will decrease. The characteristic inverse time for a channel is $f_* = \tau_{\mathrm{op}}^{-1} + \tau_{\mathrm{cl}}^{-1}$, where τ_{cl} is the average closed time of the channel. With only one type of channel present in a cell, there will be a sigmoidally shaped, Lorentzian noise spectrum with an inflection point at $f = f_*$. With many types of channels for different kinds of ions present it is indeed possible to obtain a $1/f$ spectrum over several decades as the sum of Lorentzians [86].

To obtain the voltage power spectral density, we have to multiply $S_I^{\text{noneq}}(f)$ by R^2, where R represents the electrical resistance of the entire cell membrane. We let the cell surface area measure A. So we have $S_V^{\text{noneq}}(0) \approx 4\,Ne\,\langle I\rangle\,R^2$. The equilibrium Nyquist voltage noise across the same cell membrane is $S_V^{\text{eq}}(f) \approx 4kTR$. This is white noise and has the same strength at all frequencies. We thus obtain the following formula at $f = 0$ for the ratio $\theta(0)$ of the nonequilibrium noise and the equilibrium noise:

$$\theta(0) \approx \frac{Ne\langle I\rangle R}{kT} \tag{7.16}$$

The transmembrane current $\langle I\rangle$ is proportional to the cell surface A. The resistance R is inversely proportional to A. So eventually, the cell surface area and the cell geometry in general cancel out of the equation.

Data for the steady-state Na^+ flux through several types of cell membranes (e.g., rat soleus, sheep purkinje, squid axon, guinea pig auricles, and frog sartorius) are available [90]. That flux is about 50 pmol/(cm^2 sec). The vast majority of transmembrane ion transport is carried out by Na,K-ATPase, which transports two K^+ ions for every three Na^+ ions. We assume Na^+ and K^+ transport to therefore be about equal. After multiplying by Faraday's constant (the number of coulombs in a mole, i.e., about 10^5), we get a total current of about $\langle I\rangle \approx 10\ \mu A/cm^2$. The resistance of a cell membrane varies from 10^3 Ω cm^2 (squid axon) to 7×10^3 Ω cm^2 (mammalian cardiac cell). We thus find for $\theta(0)$ a value of about 5000.

Based on experimental data, it has been estimated that at 1 Hz the $1/f$ noise in the frog node of Ranvier is about a thousand times larger than thermal noise [91]. This is consistent with our estimate. Experimentally, it turns out that the power spectral density is constant from $f = 0$ up to about somewhere between 1 and 10 Hz [86,89]. At that point, the power spectral density starts to fall off as $1/f$. This means that we reach $\theta(f) = 1$, that is, the equilibrium and nonequilibrium noise being equal, somewhere near 10^4 Hz. Figure 7.5, in which the horizontal axis is in radians per second, indeed shows flattening between 10^3 and 10^4 Hz. At the 50- and 60-Hz power line frequencies, the nonequilibrium voltage noise is expected to exceed the equilibrium voltage noise by a factor of at least 10^2.

However, we should pause before taking the value of θ and employ it to incorporate nonequilibrium noise in the evaluation of a signal-to-noise ratio. As we saw earlier in this section, nonequilibrium noise may be a way to transduce energy from one stored form to another. So a signal can come in the form of a piece of nonequilibrium noise. With this gray area between signal and noise, it may no longer be straightforward to calculate a signal-to-noise ratio. There has been a natural selection toward high signal-to-noise ratios for signals whose detection has been important for the survival of the organism for many millennia. But what the signal-to-noise ratios and detection thresholds are for ELF and microwave radiation, which are relatively new phenomena in the environment, and how nonequilibrium noise figures in all of this is still open to conjecture and debate.

7.7 Chemical Noise

Chemical noise consists of both fundamental chemical noise (stochastic variations in net or accumulated amounts of a particular ion or molecule) and nonfundamental changes in chemical amount (molecular number) due to influences other than the applied field. We again adopt a recent discussion [12] in which an arbitrary biological system is considered.

In the discussion, attention focuses on weakly interacting fields that can create small chemical changes, but much of the approach is also relevant to strongly interacting fields, for example, those causing cell membrane electroporation (see Chapter 9 on electroporation in Ref. [127]). To begin, consider a small physical perturbation of the biological system due to the interaction of a local electromagnetic field, $\vec{F}_{\text{local}}(\vec{r}, t)$, that may vary from site to site within the volume of the biological system. In general, $\vec{F}_{\text{local}}$ may have a complicated dependence of its magnitude and direction on time and position, such that a formal prescription for calculating the field-induced molecular change due to an exposure is

$$\bar{n}_S = \int_{t=0}^{t=t_{\text{exp}}} \int_{\text{system volume}} J_0(t') f_{\text{bpm}}(\vec{F}_{\text{local}}(\vec{r},t')) \, dV \, dt' \tag{7.17}$$

We regard $\bar{n}_S$ as a molecular change signal. It is the primary consequence of the field exposure for the case where only one process, or one step in a cascade, is altered. Integration is carried out over the entire biological system volume and over the time comprising the exposure, t_{exp} (or control). This yields the accumulated, total chemical (molecular) change due to the applied field during the exposure. Other changes in the same ionic or molecular species may result from competing influences, for example, temperature variations, during t_{exp}.

The applied field interacts through one or more of a limited class of biophysical mechanisms. Here, *biophysical mechanism* means a class of interactions by which the field alters an ongoing biochemical rate (transport or reaction), with the rate arising from nonequilibrium processes dependent on metabolism. Examples of known biophysical mechanisms involving electric fields are heating (most biochemical processes have a nonzero temperature dependence), voltage-gated channels, electroconformational coupling of membrane enzymes, electroporation, and iontophoresis (mainly electrophoresis, but in some cases also electroosmosis). Examples involving magnetic fields are radical-pair reactions and twisting of magnetic material (magnetite or contaminant magnetic particles). As used here, a biophysical mechanism modulates an ongoing biochemical process, and both the coupling strength and the magnitude of the basal rate are important.

For a particular type of biophysical mechanism (bpm), the function f_{bpm} $(\vec{F}_{\text{local}}$ $(t))$ describes the instantaneous alteration of the basal rate, J_0, which itself can vary in time [92]. The local field can be computed numerically at the tissue level (millimeter scale; see Chapter 11 on dosimetry, this volume) [93–99] and at the cellular level [100,101]. The time and position dependence of $\vec{F}_{\text{local}}$ $(\vec{r},t)$ is often simple, namely, a constant magnitude (steady or DC) field, a constant amplitude periodic (AC) field, or at high frequencies a spatially decaying amplitude field due to power absorption. Environmental and occupational fields can be much more complicated, such that piecewise continuous representations may be needed.

If a weakly coupled physical perturbation alters the basal rate of a biochemical process (transport or reaction), the total chemical (molecular) change, expressed as the number of molecules, is

$$\bar{n} = \bar{n}_0 + \bar{n}_S \tag{7.18}$$

where $\bar{n}_0$ is the basal change during an exposure (sensing) time t_{exp}, and $\bar{n}_S$ is the (much smaller) molecular change due to the field exposure [22,45,92,102]. As noted above, $\bar{n}_S$ can be regarded as a molecular change signal. The basal process is far from equilibrium,

driven by free-energy differences associated with metabolism. The largest field-induced molecular change occurs for a steady (DC) field exposure [22,102]:

$$\bar{n}_S = K_{\text{bpm,dc}} F_0 \; J_0 \; t_{\text{exp}} \tag{7.19}$$

where $K_{\text{bpm,dc}}$ describes the alteration of the basal rate by the steady field, here of magnitude F_0. Equation 7.19 is the DC version of the case of a weakly coupled periodic perturbation, previously described for the case of an extracellular electric field [45,92], namely,

$$\bar{n}_S = K_{\text{bpm,ac}} F_0^2 \; J_0 \; t_{\text{exp}} \tag{7.20}$$

where $K_{\text{bpm,ac}}$ describes the coupling that leads to rectification of the ongoing rate [45]. For basal rates with more complicated time dependence, Equation 7.17 may need to be evaluated numerically, but the same basic ideas apply. Equation 7.20 is valid for long exposures, involving a large number of cycles of the periodic field. Basal rates that can be altered by weakly interacting electromagnetic fields by definition involve small interaction energies, so that thermal fluctuations and chemical free-energy differences result in nonzero basal rates. A zero basal rate with an extremely large activation or interaction energy cannot, therefore, be expected to be changed to a measurable nonzero rate by a weakly interacting field.

A generalized, molecular change-based signal-to-noise ratio can be constructed by estimating the ratio of primary molecular change to the combined competing changes for the same molecular (ionic) species. We consider the simplest case of the field altering the rate at one step in a single pathway but note that in principle the present analysis can be extended to include multiple steps involving more than one biochemical pathway. We further assume that this biochemical has its rate through the pathway altered slightly by a physical perturbation, here an electromagnetic field. But competing influences can also alter the rate. Such influences include temperature variations, normal physiological concentration variations, changes in hormones and other regulating biochemicals, and mechanical perturbations of cells and tissues. Competing molecular changes can also be created by a background electromagnetic field, for example, normal electrical activity within the human body or by movement in the earth's magnetic field, interacting through the same biophysical mechanism. Such competition goes beyond fundamental chemical noise (molecular shot noise). Nonionizing influences can only modulate ongoing processes, and therefore such influences cannot (essentially by definition) introduce foreign molecules. This has the important consequence that competing molecular changes may arise from several sources (Table 7.1).

TABLE 7.1

Quantities Employed in Generalized Chemical Noise

Symbol	Molecular Change	Source
S	$\bar{n}_S$	Field-induced molecular change signal
N	$\sqrt{\bar{n}} \approx \sqrt{\bar{n}_0}$	Molecular shot noise (fundamental)
V	$\bar{n}_V$	Molecular change due to temperature variations
C	$\bar{n}_C$	Molecular change due to concentration variations
I	$\bar{n}_M$	Molecular change due to mechanical interference
B	$\bar{n}_B$	Molecular change due to background fields

A generalized signal-to-noise ratio $(S/N)_{\text{gen}}$, can thus be considered. The field-induced molecular change signal, S, is thereby quantitatively compared to the several sources of competing molecular changes for the same biochemical (molecule or ion), yielding

$$(S/N)_{\text{gen}} = \frac{S}{f_{\text{com}}(N,V,C,I,B)} \tag{7.21}$$

The various competing molecular changes, which may or may not be independent, are combined to give the total competing molecular change, f_{com}. Important simplifications can be made if the various competing molecular changes can be approximated as independent and random around their mean values. In this case, f_{com} can be approximated as

$$f_{\text{com}}(N,V,C,I,B) \approx [N^2 + V^2 + C^2 + I^2 + B^2]^{1/2} \tag{7.22}$$

Alternatively, emphasizing the changes in terms of numbers of molecules,

$$f_{\text{com}}(N,V,C,I,B) \approx [\bar{n}_0 + (\Delta n_V)^2 + (\Delta n_C)^2 + (\Delta n_M)^2 + (\Delta n_B)^2]^{1/2} \tag{7.23}$$

All significant sources of competing molecular change are directly relevant.

Consistent with experimental treatment of errors as random, here we consider the special case that all the important competing molecular changes can be approximated as independent and random variations around their mean value, as this allows the competing changes to be added in quadrature (Equation 7.22). This leads to a general molecular change-based signal-to-noise ratio that involves Gaussian distributions, namely,

$$(S/N)_{\text{gen}} \approx \frac{S}{[N^2 + V^2 + C^2 + I^2 + B^2]^{1/2}} \tag{7.24}$$

Each of these competing molecular changes is discussed briefly below, with reference to Table 7.1.

As indicated in Table 7.1, $N = \sqrt{\bar{n}} \approx \sqrt{\bar{n}_0}$ is the competing molecular change due to fundamental stochastic variations in biochemical reaction and transport processes [15,45,92], which provides a fundamental, minimum molecular change noise. Fundamental chemical noise is increasingly recognized as important to understanding other aspects of biological systems, such as the circadian clock [103,104], control of genetic circuits [105,106], and bacterial chemotaxis [107].

Temperature variations within the volume of the biological system are generally expected to result in altered rates. When integrated over the system volume and over the exposure time, a contribution to the end-point molecular change is expected, because most biochemical processes have nonzero temperature dependence. Thus, $V = \bar{n}_v$ is the resulting, competing molecular change due to temperature variations [15]. Human core body temperature has daily variations of more than 1°C [108–113], and there are even larger variations in the extremities. Often *in vitro* electric and magnetic field experiments use feedback control, for instance, in temperature-regulated exposure chambers, but these typically have variations greater than about 0.01°C at one or a few temperature measurement sites. Temperature variations within the biological system itself are often inferred,

preferably by numerical models that can reasonably predict the temperature through the biological system by first predicting the specific absorption rate. During the exposure time, interfering temperature variation can be significant. To allow correction for temperature variations, the biological system should be characterized for its temperature sensitivity, and each particular apparatus should be characterized for its temperature variations for control and exposed conditions. As an example, an investigation first reporting athermal effects [114] was subsequently found to have temperature variation $\sim 0.1^{\circ}$C at temperature measurement sites [115]. Without thermal modeling of the exposure systems and the biological systems, however, larger temperature changes away from the measurement site cannot be ruled out. It is the temperature change and variation over the entire volume containing cells (or other specimens) that need to be quantitatively understood. Temperature measurement at one site, typically somewhere along the perimeter or boundary of a temperature-regulated apparatus, is generally insufficient. The measured biochemical quantity should also be characterized for its temperature sensitivity for the biological system studied, so that the expected V can be determined, to address the basic specificity question of whether an observed change is due to the field or to temperature changes [116].

Changes in concentration of biochemicals involved in a process are well known to alter the rate of a process. Relevant chemical species include substrates, products, inhibitors, etc. The competing molecular change due to one or more interfering concentration changes is $C = \bar{n}_{\mathrm{C}}$. In this case, a significant difference may exist for *in vitro* and *in vivo* experiments. Usually, only small, slow changes of chemical concentrations are expected *in vitro*, occurring, for example, through absorption or release of molecules (ions) from glass- and plasticware, spontaneous chemical decomposition, binding to cellular constituents, or evaporation. Uptake or release of interfering biochemicals from a biological preparation could be the predominant source, particularly if cells grow (taking up molecules) or die (releasing molecules). *In vivo* concentration variations are relatively large, because of normal physiologic variations. For example, Ca^{2+} concentration varies in humans by more than 1% over a day [117,118]. Unless buffered, these normal biochemical variations also compete with the field-induced molecular change.

Movement of tissue *in vivo* and vibration of an experimental apparatus containing a biological system can also create a mechanically induced molecular change, $I = \bar{n}_{\mathrm{M}}$, that competes with a molecular change signal. In this case, the competing molecular change is due to interference of mechanical stress and strain [119,120], often present at high levels in living humans [11,121,122] but at low levels for *in vitro* experiments. *In vitro* apparatus can have quite different mechanical properties and isolation from ambient vibrations. Indeed, it has been found in some experiments that mechanical vibrations create effects larger than the field exposure [123]. Tissues *in vivo* experience significant mechanical deformation, but there is the least strain expected within the bone marrow and the brain [120]. This may be relevant to the ''contact current hypothesis,'' which suggests that currents in the bone marrow may be important in exposures of children [124–126].

Background fields can, of course, also couple to biochemical processes through the same biophysical mechanisms as the applied field. Background field-induced molecular change competes, and is denoted by $B = \bar{n}_B$. Examples of background electromagnetic fields include the endogenous electrical fields generated within the body by cardiac, muscular, and neural activity and the sampling of different field values (local anomalies) in the ambient magnetic field as mobile humans move about in their environment. *In vitro* background fields will depend on the particular experimental environment, are usually small and constant, and are often measured.

7.8 Interpretation of Experiments

Specificity is fundamentally important to interpret experiments, as one wants to know what agent is responsible for the observed change(s). This is particularly relevant to experiments that find small changes in biological systems that are exposed to small electromagnetic fields. A basic challenge is to show that other influences are not responsible. Because it is well known that most biochemical processes have a significant temperature dependence, the approximate temperature sensitivity of the observed quantity should be determined or known, and some bound should be established for temperature drift or variations in the experiment. However, as already noted, even big changes can have more than one candidate cause. Both tissue electroporation and tissue movement can, for instance, underlie the changes in molecular uptake associated with large field pulses. For this reason, signal-to-noise ratio considerations should be preceeded by establishing field specificity, which can be much more difficult than observing a change associated with a field exposure. To establish specificity, a number of issues must be considered, many of which will be discussed next.

Many experiments determine quantities related to biochemical change. Exceptions are experiments that determine physical quantities such as voltages and currents, temperature changes, and magnetic particle rotation. However, electrical measurements are the most frequent physical measurement. These are incredibly important to systems of excitable cells, with experimental preparations ranging from isolated cells to electrophysiologic measurements on humans. Accumulation of charge might be measured, but probably as a voltage on a capacitance. Signal-to-noise ratio issues are still important, of course, but usually there is an important distinction: voltages and currents (rarely charge) are readily measured continuously.

A further distinction is that most experiments involving exposures to small fields use long exposure times (many seconds to hours or even days). Such experiments commonly determine biochemical quantities directly, for example, enzyme activity, or indirectly, for example, fluorescence emission from fluorescent indicators of intracellular calcium concentration. In this broad case, consideration of generalized chemical noise is relevant. Following the discussion in a recent paper [12], both the magnitude of the field perturbation and the nature and magnitude of chemical competition need to be understood. Such analysis should explicitly estimate the coupling to ongoing, far from equilibrium, metabolically driven biochemical processes and should quantitatively determine molecular changes due to competing influences. Only then can the analysis distinguish idealized conditions from *in vitro* conditions and *in vivo* conditions and then determine whether reported effects can be explained by known biophysical mechanisms.

In vivo there are several kinds of noise, and it is important to distinguish between them. Equilibrium noise comes about as a consequence of Brownian motion, that is, the random movement of molecules at finite temperature. At equilibrium, every degree of freedom takes on the same amount of energy, and equilibrium noise is therefore easy to evaluate. For a signal to exceed the equilibrium noise band, the quantitative criteria are often readily derived. Such baseline criteria can be useful when assessing the electroreception and magnetoreception that many organisms exhibit. But the nonequilibrium nature of life brings in nonequilibrium noise. When a primary molecular change is amplified through a biochemical cascade, ''amplifier noise'' is inevitable. Nonequilibrium noise appears whenever energy is dissipated, that is, when work is done. In many biological contexts the nonequilibrium noise is much more intense than the equilibrium noise. A serious complication is constituted by the fact that nonequilibrium noise, unlike equilibrium noise, is also able to perform work, that is, be a power source for an energetically uphill

process. Many biological processes may rely on the energy transduction that can be accomplished through nonequilibrium noise. The analysis of such situations poses challenges as the noise may be a signal and the signal may be noise. There is no easy general ''common denominator'' theory for nonequilibrium noise like there is for equilibrium *kT*-noise.

In a recent discussion [12], it is argued that experimental measurements can be plausibly related quantitatively to an underlying primary molecular change because of a field exposure operating through a biophysical mechanism. It is further argued that only the uncertainty in this change propagates through biochemical amplification and therefore dominates the measurement uncertainty. A more complete approach would involve traditional, independent determination of the instrumental or assay error (quantitative characterization of the experimental measurement system). After removal of the ''instrumental noise,'' the generalized signal-to-noise ratio $(S/N)_{\text{gen}}$, could be revised upward. This would allow interpretation (correction) of experimental error to estimate the uncertainty in the measured quantity itself. Assessment of combinations of biophysical mechanism models and particular exposure can then be carried out, using the most field-sensitive versions of theoretical models for the candidate biophysical mechanisms. The criterion $(S/N)_{\text{gen}} \leq 0.1$ is a very conservative basis for ruling out a particular class of biophysical mechanism for a given field exposure. Similarly, the criterion $(S/N)_{\text{gen}} \geq 10$ is a conservative basis for ruling in a candidate biophysical mechanism for a given exposure, retaining that biophysical mechanism hypothesis for further evaluation. This approach provides a quantitative basis for rejecting or accepting hypothetical biophysical mechanisms as candidate explanations for an experimental measurement.

The traditional choice $(S/N)_{\text{gen}} \approx 1$ is a useful but somewhat arbitrary dividing line, which indicates conditions for which an effect might appear. $(S/N)_{\text{gen}} \leq 0.1$ and $(S/N)_{\text{gen}} \geq 10$ provide criteria for stronger conclusions, allowing rejection or provisional retention of a biophysical mechanism hypothesis. This approach to interpreting experiments thus provides a general method for carrying out theoretical assessment of reported weak field exposure effects. This approach can distinguish relatively quiet *in vitro* conditions from *in vivo* conditions containing more and larger influences of competing molecular change. This in turn allows quantitative estimates of whether an *in vitro* result is relevant to *in vivo* conditions.

Acknowledgment

This work was supported partially by NIH grant RO1-GM63857.

References

1. G.N. Stewart. The changes produced by the growth of bacteria in the molecular concentration and electrical conductivity of culture media. *J. Exp. Med*., 4:235–243, 1899.
2. R. Eden and G. Eden. *Impedance Microbiology*. Research Studies Press, Letchworth, Herts, U.K., 1984.
3. M. Wawerla, A. Stolle, B. Schalch, and H. Eisgruber. Impedance microbiology: applications in food hygiene. *J. Food Prot*., 62:1488–1496, 1999.

4. J. McPhillips and N. Snow. Studies on milk with a new type of conductivity cell. *Aust. J. Dairy Technol*., 3:192–196, 1958.
5. T. Ritz, P. Thalau, J.B. Phillips, R. Wiltschko, and W. Wiltschko. Resonance effects indicate a radical-pair mechanism for avian magnetic compass. *Nature*, 429:177–180, 2004.
6. D. Cohen. Ferromagnetic contaminants in the lungs and other organs of the body. *Science*, 180:745–748, 1973.
7. J.L. Kirschvink, A.K. Kirschvink, and B.J. Woodford. Magnetite biomineralization in the human brain. *Proc. Natl. Acad. Sci*., 89:7683–7687, 1992.
8. J.R. Dunn, M. Fuller, J. Zoeger, J. Dobson, F. Heller, J. Ilammann, E. Caine, and B.M. Moskowitz. Magnetic material in the human hippocampus. *Brain Res. Bull*., 36:149–153, 1994.
9. P.L. McNeil and S. Ito. Molecular traffic through plasma membrane disruptions of cells. *In Vivo J. Cell Sci*., 96:549–556, 1990.
10. P.L. McNeil and R.A. Steinhardt. Loss, restoration, and maintanence of plasma membrane integrity. *J. Cell Biol*., 137:1–4, 1997.
11. P.L. McNeil and M. Terasaki. Coping with the inevitable: how cells repair a torn surface membrane. *Nat. Cell Biol*., 3:124–129, 2001.
12. T.E. Vaughan and J.C. Weaver. Molecular change signal-to-noise criteria for interpreting experiments involving exposure of biological systems to weakly interacting electromagnetic fields. *Bioelectromagnetics*, 26:305–322, 2005.
13. N.G. Van Kampen. *Stochastic Processes in Physics and Chemistry*. Elsevier, Amsterdam, 1992.
14. R.C. Duncan, R.G. Knapp, and M.C. Miller. *Introductory Biostatistics for the Health Sciences*. John Wiley & Sons, New York, 1983.
15. J.C. Weaver, T.E. Vaughan, and G.T. Martin. Biological effects due to weak electric and magnetic fields: the temperature variation threshold. *Biophys. J*., 76:3026–3030, 1999.
16. J.C. Weaver. Understanding conditions for which biological effects of nonionizing electromagnetic fields can be expected. *Bioelectrochemistry*, 56:207–209, 2002.
17. C.W. Helstrom. *Statistical Theory of Signal Detection*, Second Edition. Pergamon Press, New York, 1968.
18. A.J. Kalmijn. Electro-perception in sharks and rays. *Nature*, 212:1232–1233, 1966.
19. A.J. Kalmijn. Electric and magnetic field detection in elasmobranch fish. *Science*, 218:916–918, 1982.
20. W.J. Moore. *Physical Chemistry*. Longman, London, 1972.
21. A.J. Kalmijn. Graded positive feedback in elasmobranch ampullae of lorenzini. In S.M. Bezrukov, Ed. *Unsolved Problems of Noise and Fluctuations: UPoN 2002: Third International Conference*, volume 665 of *Conference Proceedings*, pp. 133–141, American Institute of Physics, Melville, NY, 2003.
22. R.K. Adair, R.D. Astumian, and J.C. Weaver. Detection of weak electric fields by sharks, rays, and skates. *Chaos*, 8:576–587, 1998.
23. S.M. Bezrukov. Sensing nature's electric fields: ion channels as active elements of linear amplification. In S.M. Bezrukov, Ed. *Unsolved Problems of Noise and Fluctuations: UPoN 2002: Third International Conference*, volume 665 of *Conference Proceedings*, pp. 142–149, American Institute of Physics, Melville, NY, 2003.
24. J.C. Weaver, T.E. Vaughan, and R.D. Astumian. Biological sensing of small field differences by magnetically sensitive chemical reactions. *Nature*, 405:707–709, 2000.
25. R.P. Blakemore. Magnetotactic bacteria. *Science*, 190:377–379, 1975.
26. R. Blakemore. Magnetotactic bacteria. *Annu. Rev. Microbiol*., 36:217–238, 1982.
27. J.L. Kirschvink, M.M. Walker, and C.E. Diebel. Magnetite-based magnetoreception. *Curr. Opin. Neurobiol*., 11:462–467, 2001.
28. J.L. Kirschvink. Comment on ''Constraints on biological effects of weak exteremely-low-frequency electromagnetic fields.'' *Phys. Rev. A*, 46:2178–2184, 1992.
29. M.M. Walker, T.E. Dennis, and J.L. Kirschvink. The magnetic sense and its use in long-distance navigation by animals. *Curr. Opin. Neurobiol*., 12:735–744, 2002.
30. National Institute of Environmental Health Sciences (NIEHS). NIEHS Report on Health Effects from Exposure Power-Line Frequency Electric and Magnetic Fields. NIH Publication No. 99–4493, 1999.

31. R.K. Adair. Effects of ELF magnetic fields on biological magnetite. *Bioelectromagnetics*, 14:1–4, 1993.
32. C. Polk. Effects of extremely-low-frequency magnetic fields on biological magnetite. *Bioelectromagnetics*, 15:261–270, 1994.
33. R.K. Adair. Constraints on biological effects of weak extremely-low-frequency electromagnetic fields. *Phys. Rev. A*, 43:1039–1048, 1991.
34. K.R. Foster and H.P. Schwan. Dielectric properties of tissues and biological materials: a critical review. *CRC Crit. Rev. Bioeng*., 17:25–104, 1989.
35. J.B. Johnson. Thermal agitation of electricity in conductors. *Phys. Rev*., 32:97–109, 1928.
36. H. Nyquist. Thermal agitation of electric charge in conductors. *Phys. Rev*., 32:110–113, 1928.
37. W. Schottky. Über spontane stromschwankungen in verschiedenen elektrizitätsleitern. *Ann. Phys. (Leipzig)*, 57:541–568, 1918.
38. R. Sarpeshkar, T. Delbrück, and C.A. Mead. White noise in MOS transistors and resistors. *IEEE Circuits Devices*, Nov.:23–29, 1993.
39. M. Bier. Gauging the strength of power frequency fields against membrane electrical noise. *Bioelectromagnetics*, 26:595–609, 2005.
40. B. Hille. *Ion Channels of Excitable Membranes*. Sinauer, Sunderland, MA, 1992.
41. P. Läuger. *Electrogenic Ion Pumps*. Sinauer, Sunderland, MA, 1991.
42. J.C. Weaver and R.D. Astumian. The response of living cells to very weak electric fields, the thermal noise limit. *Science*, 247:459–462, 1990.
43. W.T. Kaune. Thermal noises limit on the sensitivity of cellular membranes to power frequency electric and magnetic fields. *Bioelectromagnetics*, 23:622–928, 2002.
44. G. Vincze, N. Szasz, and A. Szasz. On the thermal noise limit of cellular membranes. *Bioelectromagnetics*, 26:28–35, 2005.
45. R.D. Astumian, J.C. Weaver, and R.K. Adair. Rectification and signal averaging of weak electric fields by biological cells. *Proc. Natl. Acad. Sci*., 92:3740–3743, 1995.
46. L. Brillouin. Can the rectifier become a thermodynamical demon? *Phys. Rev*., 78:627–628, 1950.
47. P.W. Bridgman. Note on the principle of detailed balancing. *Phys. Rev*., 31:101–102, 1928.
48. R.C. Tolman. The principle of microscopic reversibility. *Proc. Natl. Acad. Sci*., 11:436–439, 1925.
49. R.P. Feynman, R.B. Leighton, and M. Sands. *The Feynman Lectures on Physics*. Addison-Wesley, Reading, MA, 1966.
50. M. von Smoluchowski. Experimentell nachweisbare, der üblichen thermodynamik widersprechende molekularphänomene. *Phys. Zeitschr*., 13:1069–1080, 1912.
51. P.W. Atkins. *The Second Law*. Scientific American Books, New York, 1984.
52. H.S. Leff and A.F. Rex, Eds. *Maxwell's Demon: Entropy, Information, Computing*. Princeton University Press, Princeton, NJ, 1990.
53. J. Howard and A.J. Hudspeth. Compliance of the hair bundle associated with gating of mechanoelectrical transduction channels in the bullfrog's saccular hair cell. *Neuron*, 1:189–199, 1988.
54. M. Magnasco. Forced thermal ratchets. *Phys. Rev. Lett*., 71:1477–1480, 1993.
55. M. Bier. Brownian ratchets in physics and biology. *Contemp. Phys*., 38:371–379, 1997.
56. R.D. Astumian and M. Bier. Fluctuation driven ratchets: molecular motors. *Phys. Rev. Lett*., 72:1766–1769, 1994.
57. R.D. Astumian. Thermodynamics and kinetics of a brownian motor. *Science*, 276:917–922, 1997.
58. M. Bier and R.D. Astumian. Biased Brownian motion as the operating principle for microscopic engines. *Bioelectrochem. Bioenerg*., 39:67–75, 1996.
59. I. Kosztin and K. Schulten. Fluctuation-driven molecular transport through an asymmetric membrane channel. *Phys. Rev. Lett*., 93:238102-1–238102-4, 2004.
60. Z. Siwy, I.D. Kosińska, and A. Fuliński. On the validity of continuous modelling of ion transport through nanochannels. *Europhys. Lett*., 67:683–689, 2004.
61. Z. Siwy, I.D. Kosińska, A. Fuliński, and C.R. Martin. Asymmetric diffusion through synthetic nanopores. *Phys. Rev. Lett*., 94:048102-1–048102-4, 2005.
62. Z. Siwy and A. Fuliński. Fabrication of a synthetic nanopore ion pump. *Phys. Rev. Lett*., 89:198103-1–198103-4, 2002.

63. J. Bernamont. Fluctuations in the resistance of thin films. *Proc. Phys. Soc*., 49:138–139, 1937.
64. B. Pellegrini, R. Saletti, P. Terreni, and M. Prudenziati. $1/f^{\gamma}$ noise in thick-film resistors as an effect of tunnel and thermally activated emissions, from measures versus frequency and temperature. *Phys. Rev. B*, 27:1233–1243, 1983.
65. J.B. Bassingthwaighte, L.S. Liebovitch, and B.J. West. *Fractal Physiology*. Oxford University Press, New York, 1994.
66. C. Wunsch. Bermuda sea level in relation to tides, weather, and baroclinic fluctuations. *Rev. Geophys*., 10:1–49, 1972.
67. M. Dishon-Berkovits and R. Berkovits. Work-related tardiness: lateness incident distribution and long-range correlations. *Fractals*, 5:321–324, 1997.
68. P. Bak, C. Tang, and K. Wiesenfeld. Self-organized criticality: an explanation of $1/f$ noise. *Phys. Rev. Lett*., 59:381–384, 1987.
69. P. Bak. *How Nature Works*. Springer-Verlag, New York, 1996.
70. S. Kauffman. *Investigations*. Oxford University Press, New York, 2000.
71. B.D. Malamud, G. Morein, and D.L. Turcotte. Forest fires: an example of self-organized critical behavior. *Science*, 281:1840–1842, 1998.
72. H.M. Jaeger, C. Liu, and S.R. Nagel. Relaxation at the angle of repose. *Phys. Rev. Lett*., 62:40–43, 1989.
73. S. Nagel. Instabilities in a sandpile. *Rev. Mod. Phys*., 64:321–325, 1992.
74. M. Bretz, J.B. Cunningham, P.L. Kurczynski, and F. Nori. Imaging of avalanches in granular materials. *Phys. Rev. Lett*., 69:2431–2434, 1992.
75. J.G. Nicholis, A.R. Martin, and B.G. Wallace, Eds. *From Neuron to Brain*. Sinauer, Sunderland, MA, 1992.
76. H.E. Derksen and A.A. Verveen. Fluctuations of resting neural membrane potential. *Science*, 151:1388–1389, 1966.
77. H.E. Derksen. Axon membrane voltage fluctuations. *Acta Physiol. Pharmacol. Neerl*., 13:373–466, 1965.
78. H.E. Derksen and A.A. Verveen. Fluctuations in membrane potential of axons and the problem of coding. *Kybernetik* 2:152–160, 1965.
79. D. Colquhoun and A.G. Hawkes. On the stochastic properties of bursts of single ion channel openings and of clusters of bursts. *Philos. Trans. R. Soc. Lond*., 300:1–59, 1982.
80. S.D. Silberberg and K.L. Magleby. Preventing errors when estimating single channel properties from the analysis of current fluctuations. *Biophys. J*., 65:1570–1584, 1993.
81. D. Colquhoun, C. Hatton, and A.G. Hawkes. The quality of maximum likelihood estimation of ion channel rate constants. *J. Physiol. (Lond.)*, 547:699–728, 2003.
82. L.S. Liebovitch, J. Fishbarg, and J.P. Koniarek. Ion channel kinetics: a model based on fractal scaling rather than multistate Markov processes. *Math. Biosci*., 84:37–68, 1987.
83. L.S. Liebovitch. Analysis of fractal ion channel gating kinetics: kinetic rates, energy levels, and activation energies. *Math. Biosci*., 93:97–115, 1989.
84. L.S. Liebovitch. Testing fractal and Markov models of ion channel kinetics. *Biophys. J*., 55:373–385, 1989.
85. I. Goychuk and P. Hänggi. Fractional diffusion modeling of ion channel gating. *Phys. Rev. E*, 70:051915-1–051915-9, 2004.
86. K. Diba, H.A. Lester, and C. Koch. Intrinsic noise in cultured hippocampal neurons: experiment and modeling. *J. Neurosci*., 24:9723–9733, 2004.
87. S.M. Bezrukov and M. Winterhalter. Examining noise sources at the single molecule level: $1/f$ noise of an open maltoporin channel. *Phys. Rev. Lett*., 85:202–205, 2002.
88. Z. Siwy and A. Fuliński. Origin of $1/f^{\alpha}$ noise in membrane channel currents. *Phys. Rev. Lett*., 89:158101-1–158101-4, 2002.
89. L.J. DeFelice. *Introduction to Membrane Noise*. Plenum Press, New York, 1981.
90. O.M. Sejersted. Maintenance of Na,K-homeostasis by Na,K-pumps in striated muscle. *Prog. Clin. Biol. Res*., 268B:195–206, 1988.
91. F.S. Barnes. Interaction of DC and ELF electric fields with biological materials and systems. In C. Polk and E. Postow, Eds. *Handbook of Biological Effects of Electromagnetic Fields*, pp. 103–147, CRC Press, Boca Raton, FL, 1996.

92. J.C. Weaver, T.E. Vaughan, R.K. Adair, and R.D. Astumian. Theoretical limits on the threshold for the response of long cells to weak ELF electric fields due to ionic and molecular flux rectification. *Biophys. J.*, 75:2251–2254, 1998.
93. M. Stuchly and T. Dawson. Interaction of low-frequency electric and magnetic fields with the human body. *Proc. IEEE*, 88:643–662, 2000.
94. M.A. Stuchly and O.P. Gandhi. Inter-laboratory comparison of numerical dosimetry for human exposure to 60 Hz electric and magnetic fields. *Bioelectromagnetics*, 21:167–174, 2000.
95. P.A. Mason, W.D. Hurt, T.J. Walters, J.A. D'Andrea, P. Gajšek, K.I. Ryan, D.A. Nelson, K.I. Smith, and J.M. Ziriax. Effects of frequency, permittivity and voxel size on predicted specific absorption rate values in biological tissue during electromagnetic-field exposure. *IEEE Trans. Microwave Theory Technol.*, 48:2050–2058, 2000.
96. P. Gajsek, T.J. Walters, W.D. Hurt, D.A. Nelson, and P.A. Mason. Empirical validation of SAR values predicted by FDTD modeling. *Bioelectromagnetics*, 23:37–48, 2002.
97. M. Nadeem, T. Thorlin, O.P. Gandhi, and M. Persson. Computation of electric and magnetic stimulation in human head using the 3-D impedance method. *IEEE Trans. Biomed. Eng.*, 50:900–907, 2003.
98. T.W. Dawson, K. Caputa, M.A. Stuchly, and R. Kavet. Comparison of electric fields induced in humans and rodents by 60-Hz contact currents. *IEEE Trans. Biomed. Eng.*, 50:744–753, 2003.
99. S.J. Allen, E.R. Adair, K.S. Mylacraine, W. Hurt, and J. Ziriax. Empirical and theoretical dosimetry in support of whole body radio frequency (RF) exposure in seated human volunteers at 220 MHz. *Bioelectromagnetics*, 26:440–447, 2005.
100. T.R. Gowrishankar and J.C. Weaver. An approach to electrical modeling of single and multiple cells. *Proc. Natl. Acad. Sci.*, 100:3203–3208, 2003.
101. D.A. Stewart, T.R. Gowrishankar, and J.C. Weaver. Transport lattice approach to describing cell electroporation: use of a local asymptotic model. *IEEE Trans. Plasma Sci*, 32:1696–1708, 2004.
102. P.C. Gailey. Membrane potential and time required for detection of weak signals by voltage-gated ion channels. *Bioelectromagnetics*, 20:102–109, 1999.
103. N. Barkai and S. Liebler. Circadian clocks limited by noise. *Nature*, 403:267–268, 2000.
104. M.B. Elowitz and S. Leibler. A synthetic oscillatory network. *Nature*, 403:335–338, 2000.
105. T.S. Gardner, C.R. Cantor, and J.J. Collins. Construction of a genetic toggle switch in *Escherichia coli. Nature*, 403:339–342, 2000.
106. A. Becskei and L. Serrano. Engineering stability in gene networks by autoregulation. *Nature*, 405:590–593, 2000.
107. T.S. Shimizu, S.V. Aksenov, and D. Bray. A spatially extended stochastic model of the bacterial chemotaxis signalling pathway. *J. Mol. Biol.*, 329:291–309, 2003.
108. H.T. Hammel. Regulation of internal body temperature. *Annu. Rev. Physiol.*, 30:641–710, 1968.
109. S.A. Rubin. Core temperature regulation of heart rate during exercise in humans. *J. Appl. Physiol.*, 62:1997–2002, 1987.
110. W.R. Keatinge, A.C. Mason, C.E. Millard, and C.G. Newstead. Effects of fluctuating skin temperature on thermoregulatory responses in man. *J. Physiol.*, 378:241–252, 1986.
111. K. Shiraki, S. Sagawa, F. Tajima, A. Yokota, M. Hashimoto, and G.L. Brengelmann. Independence of brain and tympanic temperatures in an unanesthetized human. *J. Appl. Physiol.*, 65:482–486, 1988.
112. P. Webb. Temperatures of skin, subcutaneous tissue, muscle and core in resting men in cold, comfortable and hot conditions. *Eur. J. Appl. Physiol.*, 64:471–476, 1992.
113. R.K. Adair. Biophysical limits on athermal effects of RF and microwave radiation. *Bioelectromagnetics*, 24:39–48, 2003.
114. D. de Pomerai, C. Daniells, H. David, J. Allan, I. Duce, M. Mutwakil, D. Thomas, P. Sewell, J. Tattersall, D. Jones, and P. Candido. Non–thermal heat-shock response to microwaves. *Nature*, 405:417–418, 2000.
115. D.I. de Pomerai, B. Smith, A. Dawe, K. North, T. Smith, D.B. Archer, I.R. Duce, D. Jones, and E.P.M. Candido. Microwave radiation can alter protein conformation without bulk heating. *FEBS Lett.*, 543:93–97, 2003.

116. Y.L. Zhao, P.G. Johnson, G.P. Jahreis, and S.W. Hui. Increased DNA synthesis in INIT/10$T_{1/2}$ cells after exposure to a 60 Hz magnetic field: a magnetic-field or a thermal effect? *Radiat. Res.*, 151:201–208, 1999.
117. B. Morrison, A. Shenkin, A. McLelland, D.A. Robertson, M. Barrowman, S. Graham, G. Wuga, and K.J. Cunningham. Intra-individual variation in commonly analyzed scrum constituents. *Clin. Chem.*, 25:1799–1805, 1979.
118. M.G. Weyer and H. Lommel. *LONG I: Eine Longitudinal-Studie über individuelle Normbereiche, individuelle Standardbereiche, statislische Normbereiche für Prävention und Früherkennung*. Verlag Kirchheim, Mainz, 1981.
119. T.E. Vaughan and J.C. Weaver. Energetic constraints on the creation of cell membrane pores by magnetic particles. *Biophys. J.*, 71:616–622, 1996.
120. T.E. Vaughan and J.C. Weaver. Molecular change due to biomagnetic stimulation and transient magnetic fields: mechanical interference constraints on possible effects by cell membrane pore creation via magnetic particles. *Bioelectrochem. Bioenerg.*, 46:121–128, 1998.
121. P.L. McNeil. Cell wounding and healing. *Am. Sci.*, 79:222–235, 1991.
122. D. Bansal, K. Miyake, S.S. Vogel, S. Groh, C.C. Chen, R. Williamson, P.L. McNeil, and K.P. Cambell. Defective membrane repair in dysferlin-deficient muscular dystrophy. *Nature*, 423:129–131, 2003.
123. U. Valtersson, K. Hanssson Mild, and M.-O. Mattsson. Uncharacterized physical parameters can contribute more than magnetic field exposure to ODC activity *in vitro*. In F. Bersani, Ed. *Electricity and Magnetism in Biology and Medicine*, pp. 449–452, Plenum Press, New York, 1999.
124. R. Kavet, L. Zaffanella, J. Daigle, and K. Ebi. The possible role of contact current in cancer risk associated with residential magnetic fields. *Bioelectromagnetics*, 21:538–553, 2000.
125. R. Kavet, L.E. Zaffenella, R.L. Pearson, and J. Dallaplazza. Association of residential magnetic fields with contact voltages. *Bioelectromagnetics*, 25:530–536, 2004.
126. R. Kavet. Contact current hypothesis: summary of results to date. *Bioelectromagnetics*, suppl. 7:S75–S85, in press.
127. J.C. Weaver, Y. Chizmadzhev, Electroporation. In F.S. Barnes and B. Greenebaum, *Biological and Medical Aspects*, Eds. Taylor & Francis, Boca Raton, FL, Chapter 9, 2006.